Journal of Circular Economy (2026) 4:1, 265-291
https://doi.org/10.55845/joce-2026-41256

RESEARCH ARTICLE

Analysis of Lime Mortars Modified with Polymeric Waste Aggregates as a Circular Economy Strategy for Sand Replacement

Alejandra Vidales-Barriguete[1*], Daniel Ferrández[1*], Evangelina Atanes-Sánchez[2], José A. Capitán[3]

Received: 2. January 2026 / Accepted: 1. February 2026 / Published: 9. February 2026

Abstract

Currently, plastic waste is a major environmental problem. In line with circular economy principles, plastics' non-biodegradability, high volume and health impacts demand end-of-life recovery and recycling solutions. This study evaluates the use of plastic aggregates from medium-voltage cable waste in hydraulic lime mortars as a circular alternative to linear "take–make–dispose" practices. Substituting natural sand with secondary plastic aggregates conserves primary mineral resources, closes material loops for post-consumer plastics, and situates this strategy higher in the waste hierarchy than landfilling or energy recovery.

The research evaluates the replacement of natural sand with these secondary raw materials and its influence on the physicochemical and mechanical performance of mortars. Replacement levels up to 100% of the aggregate were assessed, achieving reductions in apparent density of hardened mortars of up to 30.8%. Mechanical properties were monitored at 28, 90, and 180 days, revealing a progressive gain in strength over time and showing how increasing plastic aggregate content reduces flexural and compressive strength. This mechanical evolution was correlated with changes in mineralogical composition through thermogravimetric analysis and X-ray diffraction, quantifying the gradual transformation of portlandite into calcite.

The results demonstrate that plastic waste from electrical installations can be successfully incorporated into non-structural lime-based materials, providing a valorization route for this waste stream. The study strengthens the circularity of construction products and helps reduce the consumption of natural raw materials in the building sector, offering insights for the design of sustainable mortars and contributing to a more circular management of plastic waste in construction.

Keywords Lime Mortars · Aggregates · Plastic Waste · Circular Economy · Sustainable Construction

1. Introduction

In the framework of the circular economy (CE), the construction sector is considered a priority field for closing material loops, reducing the consumption of virgin resources, and minimizing waste generation. Compared to the linear "take–make–dispose" model, CE promotes strategies such as closed-loop material cycles, industrial symbiosis, and waste-to-resource approaches, in which waste from one sector becomes a resource for another (Fritz Benachio et al., 2020; Ghaffar et al., 2020; López Ruiz et al., 2020; Ogunmakinde, 2024). Within this

* Corresponding Authors: alejandra.vidales@upm.es and daniel.fvega@upm.es
[1] Universidad Politécnica de Madrid, Escuela Técnica Superior de Edificación, Departamento de Tecnología de la Edificación, Spain
[2] Universidad Politécnica de Madrid, Escuela Técnica Superior de Ingeniería y Diseño Industrial, Spain
[3] Universidad Politécnica de Madrid, Escuela Técnica Superior de Edificación, Departamento de Matemática Aplicada y Grupo de Sistemas Complejos, Spain

context, plastic waste from electrical cables represents an underutilized stream, despite its potential for reincorporation into construction products (Lamba et al., 2021; Merlo et al., 2020; Zulkernain et al., 2021). However, current circular economy research on plastic valorization in the built environment has primarily focused on more homogeneous waste streams (e.g., packaging and end-of-life tires), largely leaving unexplored the specific performance, processing limitations, and design implications of cable-derived plastics in mineral binders.

Global plastic production has increased 200-fold between 1950 and 2015, and figures are expected to double by 2050 (Ahmed, 2023). In this context, the current volume of polymeric materials generated annually across the world is estimated at 370 million tons (Xue et al., 2023). This represents an excessive consumption of resources and implies a major environmental impact caused by the large amount of plastic waste accumulated in terrestrial and marine ecosystems (Ferrández et al., 2025). Furthermore, this waste is characterized by its slow degradation process and the large volumes occupied in landfills (Geng et al., 2022; Meng et al., 2023), having a recycling and recovery ratio of less than 10% of all global plastic production (Tejaswini et al., 2022).

Of the wide variety of plastic waste generated, this innovative study focuses on the recovery of waste produced by the sheathing of low-voltage electrical cables. Low-voltage electrical cables are made up of three parts: the cover (optional), insulation, and conductor. The cover and insulation are usually polymeric materials with a less widespread recycling and recovery process than metallic conductors (Wang et al., 2022). The treatment of the waste from this plastic cable is a critical issue, with landfill disposal, incineration, and energy recovery being the main management strategies currently used (Abadian & Russell, 2024; Ferrández et al., 2025; Meng et al., 2023; Xue et al., 2023). All of these techniques are highly polluting, given that they may generate microplastics and emit harmful gases into the atmosphere (García-Gutiérrez et al., 2025; Kulas et al., 2023). Therefore, this study suggests a more sustainable model of recovery of these solid waste products. By crushing them, lightweight aggregates are formed that can be reincorporated in the manufacturing of new sustainable construction materials, according to circular economy criteria (Syed Nasir & Qureshi, 2025).

Although examples exist of the application of plastic aggregates as a partial replacement of natural aggregates in the manufacture of masonry mortars (Lazorenko et al., 2022; Mohamad et al., 2024), no references have been found regarding the application of shredded electrical cable waste in the manufacturing of hydraulic lime mortars. In general terms, the incorporation of this type of plastic waste together with conglomerating construction materials allows for a reduction of the final density of hardened mortars (Chen et al., 2023), decreasing their thermal conductivity (Aldaou et al., 2025) and improving their behavior in response to the action of water and increasing their acoustic performance (Herrero et al., 2013; Vidales-Barriguete et al., 2020). On the other hand, as a counterpart, this type of plastic aggregate reduces the mechanical resistance to the bending and compression of mortars (Rathore et al., 2021), compromising its durability and, at times, displaying poor adhesion between the residue and the cementitious matrix (Aattache, 2022; Merlo et al., 2020). These eco-friendly materials have a wide field of application in the production of prefabricated pieces for modular construction (Zaragoza-Benzal et al., 2023).

In this research, traditional hydraulic lime mortars are chosen as an alternative to cement mortars, given that they offer a more environmentally friendly manufacturing process and the ability to absorb CO_2 during setting (Amenta et al., 2017; Meddah et al., 2023). Although hydraulic lime mortars were commonly used prior to the introduction of Portland cement over the late 19th century, currently, their use is once again being recovered for use in renovation work on buildings and historic monuments. It is also being used in the production of more sustainable prefabricated elements and coatings (Apostolopoulou et al., 2021; Hamieh et al., 2024). As relevant properties, hydraulic lime mortars are characterized by their plasticity in the fresh state and their ease of application as a coating with good hygrothermal regulation capacity (Moletti et al., 2023). It is a construction material that, in the hardened state, is a material with low surface hardness and relatively low flexural and compressive strengths (Tang et al., 2023). However, its hardening process improves mechanical resistance over time with the progressive formation of $CaCO_3$ (Athira & Manohar, 2023). On the other hand, as an additional advantage of this type of masonry mortar, its excellent chemical and physical compatibility with other construction materials stands out, which is especially useful for restoration work in historic buildings (Loureiro et al., 2020).

The major challenge posed by this research project is to encourage the use of plastic waste for the manufacture of hydraulic lime mortars. This will reduce the demand for natural aggregates in construction, as the second most consumed natural resource on the planet (Ferrández et al., 2023). Several investigations have tried to replace this type of natural aggregate with others of ceramic or concrete origins in the manufacture of

lime mortars (Raeis Samiei et al., 2015; Stefanidou et al., 2014). They have obtained materials producing a lower carbon footprint that are optimal for use as masonry materials (Resende et al., 2024). Other research shows how the incorporation of industrial micro-cork waste with anti-fungal properties improves the durability of these masonry mortars, in addition to obtaining lighter materials (Jerónimo et al., 2020). Moreover, the addition of plastic waste such as fibers from End-of-Life Tires produces lime mortars without reducing mechanical properties, with additions of up to 0.25% in volume (Gil et al., 2016). Finally, other studies have examined the effect of the partial replacement of natural aggregate with granular Polyvinyl chloride (PVC) waste in the manufacture of mortars. This led to lower water absorption by capillarity and greater thermal resistance, although there were reductions of almost 50% in the mechanical properties of the hardened mortars (Aciu et al., 2018).

This study is situated within these frameworks by assessing the use of plastic aggregates derived from medium-voltage cables in hydraulic lime mortars as a circular solution that goes beyond simple material substitution. First, it explores their technical feasibility and scalability in non-structural applications, supporting the sector's transition toward low-carbon, high-recycled-content materials in buildings (Al-Noaimat et al., 2025; Merlo et al., 2020; Norouzi et al., 2021; Zulkernain et al., 2021). Second, it generates evidence to inform the design of policies and strategies for construction and demolition waste management, aligned with circular economy objectives and built-environment decarbonization agendas (Ginga et al., 2020; López Ruiz et al., 2020; Purchase et al., 2022).

To date, no studies have been identified that evaluate the feasibility of recovering plastic waste from low-voltage electrical cables as a replacement for natural sand in mortar production. In contrast, its incorporation into gypsum-based composites has already been demonstrated, with previous work showing that this waste stream enables lightweight prefabricated elements with mechanical strength above current regulatory requirements and good water resistance (Vidales Barriguete et al., 2018; Vidales-Barriguete et al., 2020).

This paper tackles a central knowledge gap in circular-economy-oriented construction materials: although numerous investigations have examined the addition of plastic waste to mortars and concretes, there is still scarce quantitative evidence on performance–circularity trade-offs, especially regarding mechanical response and long-term durability at high substitution levels of secondary plastic aggregates.

The present study directly addresses this gap by progressively replacing natural sand with plastic aggregates derived from medium-voltage cable waste (up to 100%) in hydraulic lime mortars and assessing the impact on time-dependent mechanical behaviour, microstructural and mineralogical evolution, and density reduction. By explicitly relating these mechanical and physicochemical changes to circularity gains (valorization of a difficult-to-recycle waste stream and reduced use of virgin aggregate), the work defines the limits within which such mortars can be developed without compromising functional performance, thus supplying the missing evidence needed for CE-oriented design of non-structural building products.

Accordingly, the study characterizes the physicochemical and mechanical properties of hydraulic lime mortars incorporating recycled cable-derived plastic as lightweight aggregate, through an experimental program with different replacement ratios of natural sand. The objective is to provide a robust characterization of these more sustainable materials within a clear circular-economy framework, exploring strategies to recover plastic waste from buildings and reincorporate it into new construction products while assessing its potential scalability in widespread non-structural applications such as interior renders, plasters and non-load-bearing masonry units.

By lowering virgin sand demand and increasing recycled content in conjunction with the lower embodied energy and CO_2 uptake capacity of hydraulic lime binders, the proposed mortars promote closed-loop material cycles and support the transition toward low-carbon, high-recycled-content construction materials. At the same time, valorizing cable-derived plastic waste in mortars offers a concrete example of circular construction practice—aligned with waste-to-resource strategies—that can inform waste-management policies and future regulations aimed at boosting recycled content and closing material loops in the built environment.

2. Materials and methods

2.1. Materials

Hydraulic lime mortars were selected because they align better with circular economy and sustainability goals than purely cement-based alternatives. Lime binders have a substantially lower embodied energy and carbon footprint than Portland cement and can reabsorb a large share (up to ~90%) of the CO_2 emitted during calcination through carbonation over their service life, effectively acting as a partial carbon sink (Malathy et al., 2023; Nassiri et al., 2024; Vanderschelden et al., 2024).

In this study, the materials used for sample creation were (Figure 1):

Figure 1. (Left) lime (Center) aggregate. (Right) plastic cable waste. Source: author's own creation

- Natural hydraulic lime i.design CALIX NHL 3.5 white, which comes from the calcination of a marly limestone, subsequently slaked. It should be noted that it sets and hardens with water and then carbonates with CO_2 in the air. It is manufactured in accordance with the EN-459-1 standard for construction limes (AENOR, 2016).
- Water from *Canal de Isabel II* (Madrid), having the technical characteristics established in standard UNE-EN 196-1 (UNE, 2018).
- Standardized river sand from a gravel pit or quarry that passes through a mesh sieve of up to 4 mm. It is characterized by a high quartz content, and it meets the requirements of standard UNE-EN 196-1 (UNE, 2018).
- Plastic cable waste (CW), which comes from the recycling of disused cables (Figure 2). They contain both thermoplastic and thermosetting polymers. Its particle size fraction is equal to or less than 3 mm. The characterization of the plastic cable waste has been reported in previous studies (Vidales Barriguete, 2019; Vidales Barriguete et al., 2018). The main findings can be summarized as follows: organic matter is the predominant component (92.6%). The presence of chlorine is most likely associated with PVC from electrical cables, while the detected copper and aluminum are attributable to metallic residues from the cables themselves. In addition, the plastic cable waste exhibits limited thermal stability, remaining stable only up to approximately 200 °C and undergoing intense degradation as the temperature increases beyond this threshold. The particle size distribution analysis indicated that the entire sample passed the 4 mm sieve, with a predominant fraction of particles between 1 and 2 mm (69.1%) and 97.5% of particles larger than 0.5 mm.

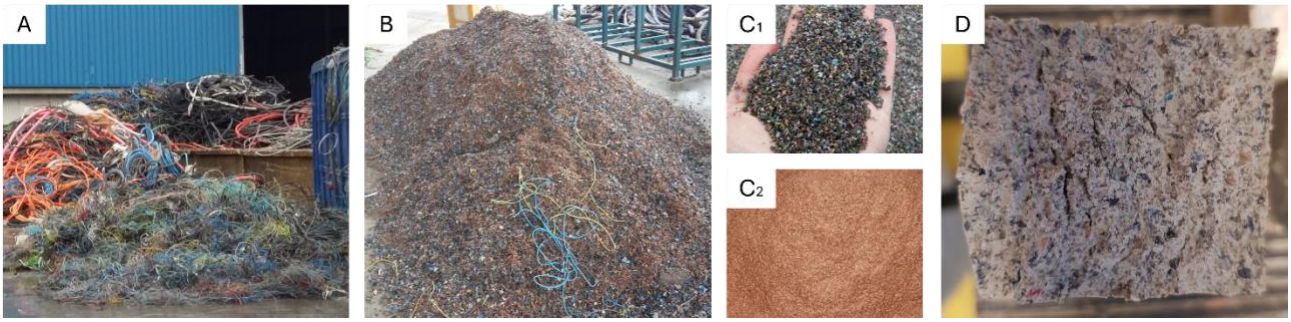

Figure 2. (A) Disused cables prepared for recycling, (B) cable shredding, materials obtained: (C1) plastic waste and (C2) copper, (D) plastic waste in lime matrix. Source: author's own creation - Lyrsa Álava

2.2. Test tube preparation

Several series of three prismatic test tubes with dimensions of 40x40x160 mm3 were produced, following the indications of standards UNE-EN 1015-2:1999/A1 and UNE-EN 196-1:2018 (AENOR, 2007; UNE, 2018). The water-to-lime mass ratio ranged from 0.9 in the specimens without residue to 0.78 in those without sand. Plastic waste, incorporated as a volumetric replacement for sand, was dosed at 25%, 50%, 75%, and 100%, as detailed in Table 1. Replacement rates up to 100% of the aggregate were considered in order to explore the upper limit of feasible material substitution under circular economy principles and to determine the point at which increased circularity—through maximizing the use of secondary plastic aggregates and reducing natural sand consumption—begins to impair the mechanical performance required for non-structural applications. Additionally, reference batches without any added residue were manufactured. All specimen series were tested at 28, 90, and 180 days.

Table 1. Composition of compounds and density

Name	Lime (g)	Water /cal	Water (g)	Sand (g)	Waste (g)	Density at 28 days (g/cm^3)	Density at 90 days (g/cm^3)	Density at 180 days (g/cm^3)
REF	450	0.90	405.0	1,350.0	0	1,981.49	2,067.12	2,103.98
CW-25%	450	0.87	391.5	1,012.5	120	1,834.32	1,887.76	1,899.37
CW-50%	450	0.84	378.0	675.0	240	1,619.58	1,676.63	1,693.00
CW-75%	450	0.81	364.5	337.5	360	1,517.08	1,556.00	1,570.92
CW-100%	450	0.78	351.0	0	480	1,370.86	1,384.47	1,401.70

During the preparation of the test tubes, the lime and the polymer residue were mixed dry for a few seconds to avoid flotation. Once the mixture was made, the water was poured in for a maximum of 10 seconds. Then the mixer was started at a slow speed. After 30 seconds, the sand was added for 30 additional seconds, and 30 more seconds of kneading at high speed were carried out. The mixer was stopped for 90 seconds to remove the mortar stuck to the walls and the bottom of the container, and, finally, mixing was continued at high speed for 60 seconds (UNE, 2018).

Once the kneading was finished, the mixture was poured into the molds, being careful to avoid the formation of air bubbles. For this, two layers were used, compacted with 60 blows each (Figure 3 left). The excess mortar was then removed, and the test tubes were placed in the humid chamber on a horizontal surface for 24 hours. Finally, the samples were removed from the mold and reintroduced into the humid chamber until 28, 90, or 180 days of curing (Figure 3 right). The conditions in the humid chamber were 20 ± 2 °C and 95-100% relative humidity, with ambient levels of CO_2, in accordance with previous studies on mortars cured with high humidity (Garijo et al., 2018; Grilo, Silva, et al., 2014).

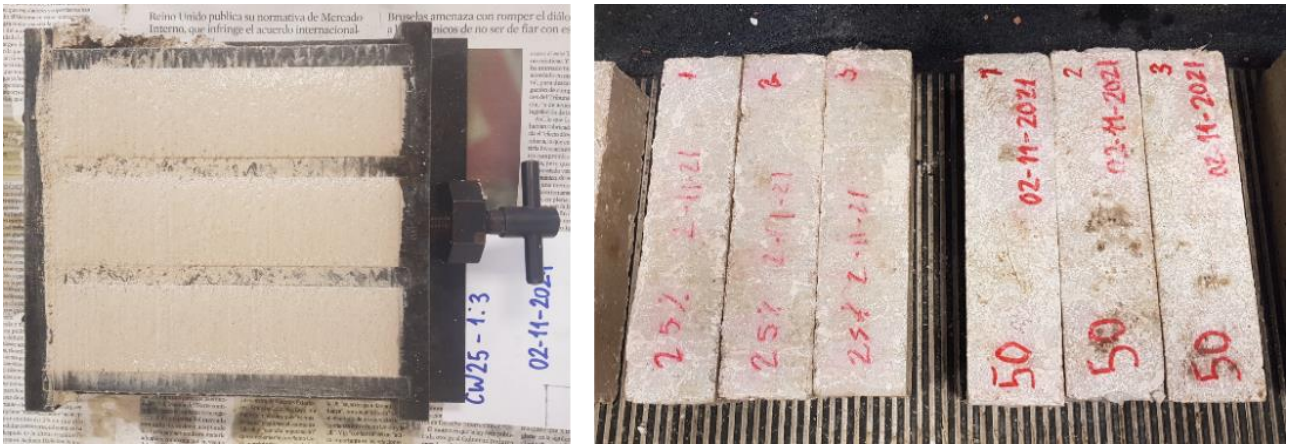

Figure 3. (Left) preparation of mixtures in molds. (Right) unmolded samples

2.3. Experimental plan

The experimental plan was carried out in two phases: one in the Chemical Analysis Laboratory of the Higher Technical School of Engineering and Industrial Design; and the other in the Materials Laboratory of the Higher Technical School of Construction, both part of the Polytechnic University of Madrid.

2.3.1. Phase 1: Physicochemical characterization of the raw material During this phase, elemental analysis, thermogravimetric analysis, and X-ray diffraction of the hydraulic lime were performed. Thermal analysis of the pellets was performed in previous investigations (Vidales Barriguete et al., 2018).

- *Elemental analysis:* It was obtained using a Bruker Fluorescence spectrophotometer, S2RANGER model with energy dispersive detector and Pd X-ray tube, using the EQUA-OXIDES measurement method. For the measurement, 9.2 g of the ground sample and 0.8 g of wax were taken.
- *Thermogravimetric analysis*: To measure the evolution of the mass as a function of temperature, dynamic gravimetric thermal analysis was performed using a TA Instruments SDT Q600 thermobalance, with a ramp ranging from room temperature to 1000°C (15°C/min) and an atmosphere of 100 ml/min of air. Thermogravimetric analysis was performed on commercial powdered lime.
- *X-ray diffraction*: was carried out using a Siemens D5000 Diffractometer, with graphite monochromator and Cu Kα (1,2) radiation. The measurement was performed on commercial powdered lime.

2.3.2. Phase 2: Physicochemical and mechanical tests on lime specimens and polymer waste The physicochemical characterization of the compounds was carried out by thermogravimetric analysis and X-ray diffraction. The porous structure of the samples was characterized via mercury porosimetry testing. Mechanical tests were performed on Shore D surface hardness, flexural strength, and compressive strength. In addition, to better understand the behavior of the mixtures in the tests, the internal structure of the compounds was observed through microscopy.

- *Thermogravimetric analysis*: the same experimental conditions were used as described in the previous section for the material, beginning, in this case, with the semi-specimens obtained after the break in the determination of the mechanical properties. The semi-specimens were dried at 60º C for 24 hours, and a sample was taken from the center of the test tube, on the side of the break. The sample was ground in an agate mortar and was sieved to 0.3 mm, in order to eliminate the residue of grain and most of the aggregate.
- *X-ray diffraction*: the same experimental conditions described in the previous section were used for the raw material. The same drying treatment of the test tubes, sampling, grinding, and sieving was carried out as described above for the thermogravimetric analysis to obtain the sample.
- *Mercury porosimetry:* the pore volume and sample distribution were determined on 28-day-old test specimens. The measurement was performed on semi-specimen pieces after they were broken using an

Autopore IV 9500 device from Micromeritics Instrument Corporation, through the introduction of mercury into the porous structure of the samples via controlled pressure. The values of bulk density (at 0.0036 MPa, minimum pressure exerted by Hg) and skeletal density (at the maximum pressure exerted by Hg on the sample in each test, 227.4929 MPa) were also calculated, in addition to the average pore diameter in volume (diameter corresponding to 50% of the volume of the total Hg introduced).

- *Shore D surface hardness (UNE-EN 13279-2 (UNE-EN 13279-2:2014, 2014):* 5 measurements were taken for each of the longitudinal lateral sides of each test tube, using a durometer to measure Shore D hardness (Figure 4a).
- *Flexural and compressive strength (UNE-EN 1015-11 (UNE, 2020):* for both tests, the Ibertest Autotest 200 work equipment was used. This equipment applied a load until a fracture occurred. The data obtained was then recorded in the computer program (Figure 4b and 4c).

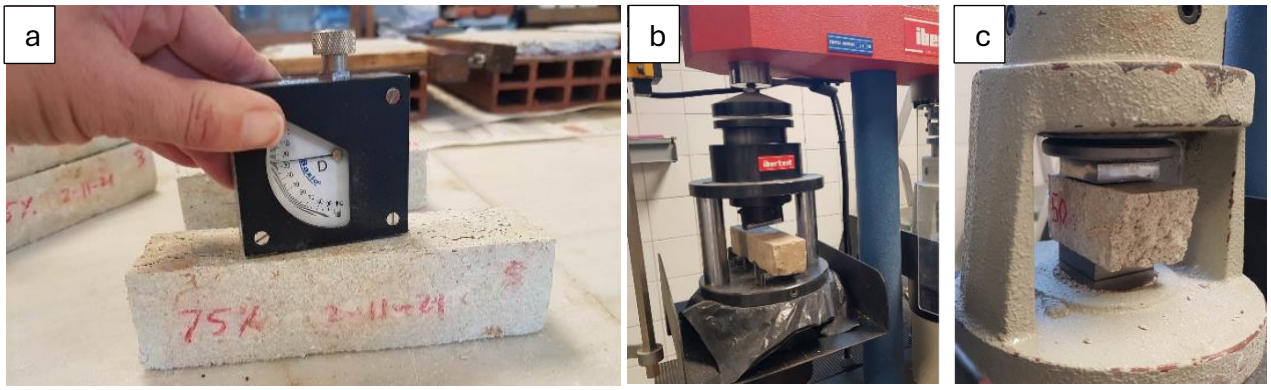

Figure 4. (a) Shore D surface hardness test; (b) Flexural strength test; (c) Compressive strength test

- *Microscopy*: to study the morphology and texture of the sample, as well as the interface between the lime and the residue, a Jeol JSM-820 scanning electron microscope operating at 20 kV was used. Cressington 108 metallizing equipment was used to prepare the samples for SEM imaging. The sample was obtained by tapping the side of one of the test tubes and selecting a piece with an interior that was as flat as possible. This newly obtained sample was coated with gold metal.

3. Results and discussion

3.1. Phase 1: Physicochemical characterization of the raw material:

3.1.1. Elemental analysis Elemental analysis of hydraulic lime was carried out using XRF (Table 2).

Table 2. Composition of the hydraulic lime (%)

CaO	SiO_2	SO_3	MgO	Al_2O_3	K_2O	Fe_2O_3	Na_2O
66.4	7.27	1.55	1.87	1.60	1.13	0.98	0.30

3.1.2. Thermogravimetric analysis The thermogravimetric analysis corresponding to the hydraulic lime binder is presented in Figure 5. In this figure, mass loss is presented as a function of temperature (green line), together with the derivative of the mass loss as a function of temperature (blue line), and the associated thermal effects as a function of temperature (brown line, with the criterion that an exothermic process is shown as an upward peak). The lime sample displays a total weight loss of approximately 15%; two clearly differentiated mass loss events are observed, both of which are endothermic. The first, between 350ºC and 500ºC, suggests a mass loss of 10.4%, and corresponds to the portlandite $Ca(OH)_2$ decomposition, giving rise to CaO and H_2O,

with the maximum in the mass derivative with the temperature (blue line) at approximately 455ºC. The second mass loss event, between 500ºC and 800ºC, corresponds to the decomposition of calcite $CaCO_3$ to give rise to CaO and CO_2, with the maximum in the mass derivative with the temperature at approximately 700ºC. Considering the stoichiometry of the decomposition reactions and mass losses, the hydraulic lime contains 42.94% portlandite and 9.96% $CaCO_3$. The results of these analyses for the polymer residue were evaluated in a previous study (Vidales Barriguete et al., 2018).

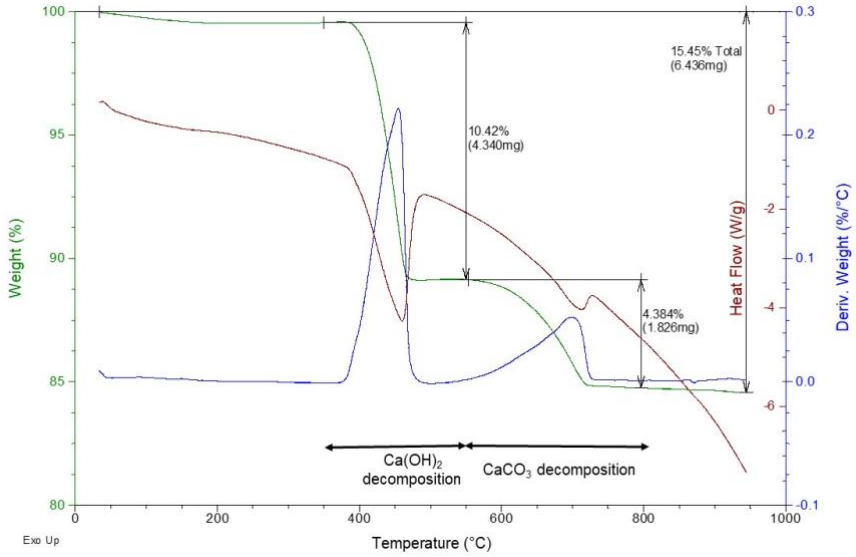

Figure 5. Thermogravimetric analysis of raw material lime

3.1.3. X-ray diffraction Figure 6 shows the results obtained in the X-ray diffractogram for lime. According to the chemical composition shown in Table 2, and in line with the JCPDS database, the phases identified by XRD (Figure 5) are portlandite ($Ca(OH)_2$) (more intense peaks at 2θ values of 18.09°, 34.09°, 47.12°, 50.8°, 54.34°, and 28.66°), calcite ($CaCO_3$) (more intense peaks at 2θ values of 29.41°, 39.4°, and 43.15°), quartz (SiO_2) (more intense peaks at 2θ values of 26.7°), and calcium silicate larnite ($Ca_2(SiO_4)$) (more intense peaks at 2θ values of 31.99°, 32.17°, 32.61°, 34.36°, and 41.23°), in accordance with that reported in the bibliography (Ferrández, Yedra, Atanes-Sánchez, et al., 2022; Lanas et al., 2004).

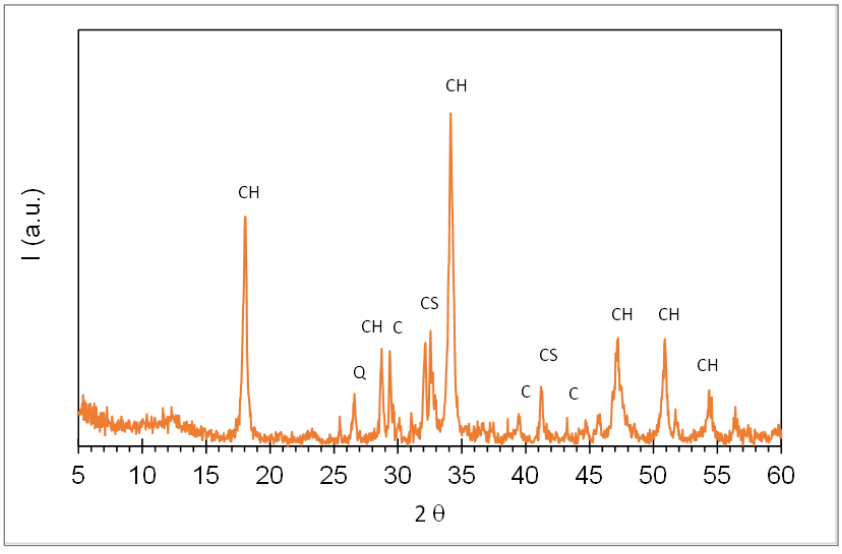

Figure 6. X-ray diffractogram of hydraulic lime. CH: portlandite. C: calcium carbonate. CS: calcium silicate. Q: quartz.

3.2. Phase 2: Tests on lime specimens and polymer waste:

With the preparation of the specimens, it was possible to verify the quantity of raw material to be used in each series, so that a reduction of up to 100% in the use of sand (complete replacement of sand volume by plastic waste) and up to 13.3% in water use was observed (Figure 7).

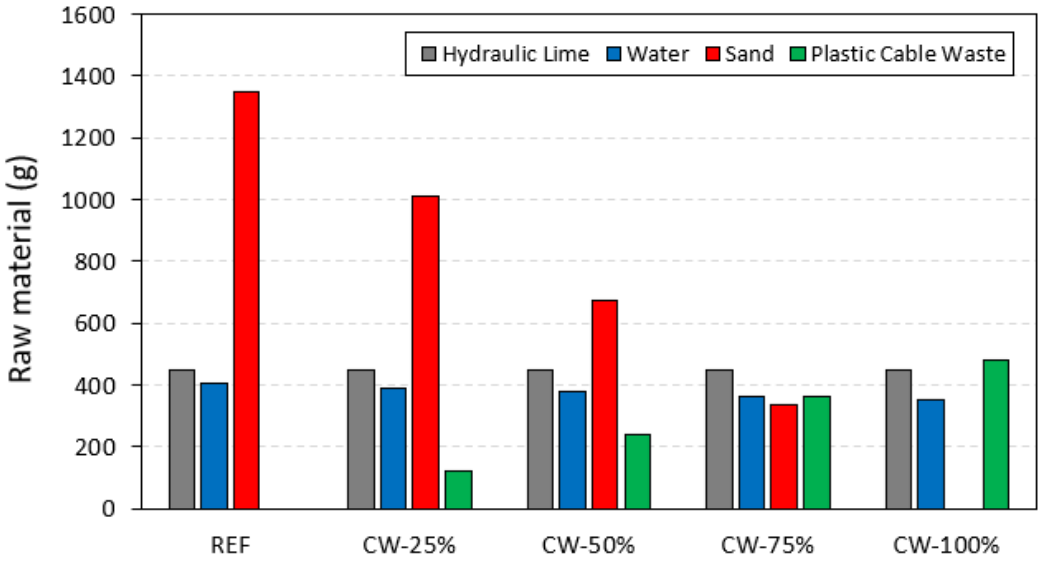

Figure 7. Raw material used in each series. Quantities required to make a 4×4×16 cm3 mold.

3.2.1. Hg porosimetry The experimental results of Hg porosimetry for the specimens after 28 days are presented in Table 3 and Figure 8. Table 3 shows the textural properties, while Figure 8 presents the cumulative and differential pore size distributions, respectively.

Table 3. Textural properties obtained from mercury porosimetry (samples at 28 days)

Name	VpHg (cm^3/g)	Bulk Density (g/cm^3)	Skeletal Density (g/cm^3)	Porosity (%)	Median pore diameter (nm)
REF	0.1773	1.7767	2.5940	31.51	289
CW-25%	0.1933	1.6616	2.4498	32.17	307
CW-50%	0.2392	1.5328	2.4221	36.72	351
CW-75%	0.3261	1.2712	2.1735	41.51	552
CW-100%	0.3774	1.0971	1.8722	41.90	627

As seen in Table 3, the pore sample volume increases as the plastic waste content increases, from 0.177 cm^3/g in the reference sample to 0.3774 cm^3/g in the sample without natural aggregate, which incorporates 100% plastic waste. The average pore diameter (obtained for the value of 50% of the pore volume) also increases as the natural aggregate is replaced with plastic waste. This result is consistent with the literature, as te partial of full replacement of natural aggregates in hydraulic lime or cement-lime mortars leads to an increase in the porosity (Iucolano et al., 2013; Merlo et al., 2021).

According to the larger pore volume, the bulk density of the samples obtained from Hg porosimetry (which includes pores and interparticle spaces) decreases as the plastic residue content increases as confirmed by other authors (Safi et al., 2013). The skeletal density values (which do not include the pore volume filled by Hg) are higher than the bulk density values. They decrease as the plastic residue content increases due to the lower density of the latter compared to both hydraulic lime and natural aggregate. It should be noted that the bulk density values obtained from Hg porosimetry are lower than those obtained for the test tubes (Table 1) since, in the test, Hg under pressure has a larger pore volume, resulting in a lower density value.

Because Hg does not penetrate the pores having diameters of less than (approximately) 4 nm, the pore volume of the samples is probably larger. This is supported by the fact that, in general, none of the accumulated pore volume curves reach a flat zone at high Hg pressure values, suggesting the presence of micropores.

Figure 8 reveals that all of the samples have a similar pore size distribution, although the pore fraction between 100 and 1000 nm shifts towards larger sizes as the proportion of plastic waste increases, in accordance with the larger average pore size presented in Table 3. The presence of micropores is also seen in Figure 8, which reveals that, as of a pore size of approximately 40 nm, the pore volume increases in the direction of that of smaller pore sizes.

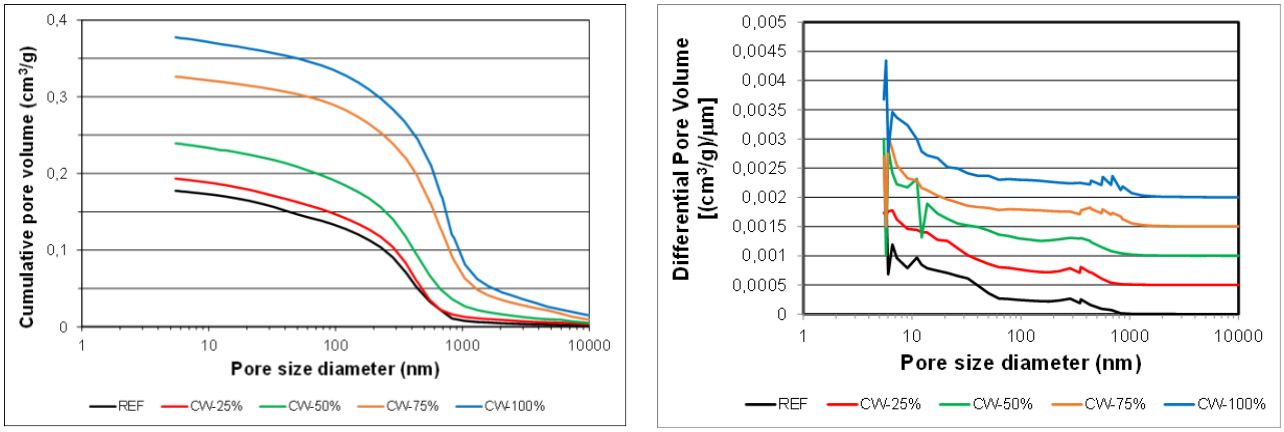

Figure 8 (left). Cumulative pore size distribution. **Figure 8 (right).** Differential pore size distribution. (Obtained by mercury porosimetry (Series VII). In the differential distribution, the curves have been shifted along the vertical axis to separate them.)

These results are consistent with the findings of several authors, with the hydraulic lime mortars showing a bimodal or multimodal pore size distribution, with most pores falling in the micropore (< 100 nm) and transition pore (100-1000 nm) ranges and porosity values around 25% (Mosquera et al., 2006; Rani et al., 2021; Zhu et al., 2019).

As will be seen later, in these lime mortars with plastic waste, the reduction in total porosity is accompanied by a weaker microstructure and interfaces, which leads to lower mechanical resistance despite having fewer pores.

3.2.2. Shore D surface hardness Figure 9 shows the results obtained in the Shore D surface hardness test, representing all the experimental values obtained. As shown in the figure, 30 measurements are reported for each age and concentration combination. It is seen that, in general, the hardness of all the samples increases as the days pass since their preparation. Specifically, the average hardness in the reference specimens at 180 days was 67% higher than at 28 days (65.20 compared to 39.03); while in the specimen with residue contents of 25%-50%-75% and 100%, at 180 days, they reached average values that were higher by 67% (54.20), 72% (49.73), 99% (46.20), and 89% (34.23), respectively, as compared to the average hardness values obtained at 28 days (32.50-28.87-23.23-18.13).

On the other hand, it can also be observed that the samples with residue presented lower hardness values as the mixture incorporated a greater amount of residue. At 28 days, the Shore D hardness of the composites with polymeric residue were reduced on average to 17%-26%-41%-54%, respectively, in CW-25%, CW-50%, CW-75%, and CW-100%, with respect to the reference sample average value (39.03). At 90 days, this downward difference in the test tubes with residues reached values of 12%-30%-40%-48% with respect to the reference average value sample (58.80). Finally, at 180 days, it settled at 17%-24%-29%-48% below the reference average value (65.20). The mean Shore D hardness values were 54.20 (CW-25%), 49.70 (CW-50%), 46.20 (CW-75%), 34.20 (CW-100%).

To statistically verify that age and residue concentration significantly affect hardness relative to the reference, and to consider their possible interaction, a two-way ANOVA was applied. The model assumes:

normally distributed errors and homoscedastic, independent errors; after fitting, these assumptions must be checked for the conclusions to be valid.

Shore D hardness was measured at several points on each specimen. To guarantee independence, only one value per test tube was used, yielding 3 × 5 × 3 = 45 observations for all age–dosage combinations. From the 10 readings taken on each tube, one was randomly selected, constructing datasets where independence (key in ANOVA) is ensured. Using the replication available, this resampling was repeated 100 times to assess the robustness of the ANOVA conclusions.

The 100% of ANOVA tests yielded significance for age and dosage separately ($p < 0.05$), confirming our conclusion that there is a statistically significant effect of dosage and age on hardness. Therefore, the results are statistically compatible with a significant effect of the concentration level of the added residue, which consistently decreases the hardness as the concentration increases, as well as on age, which increases surface hardness. The interaction term, however, was only significant, only about half of the random replicas of the dataset. This does not change the conclusion that there is a significant effect on the response variable, only informs about the interpretation of that effect because of the interaction between factors. Code and data to reproduce the statistical analyses of Shore D surface hardness data can be found at https://github.com/jcapitan-upm/polymeric_waste . We refer the reader to the data repository for the code to reproduce this analyses. Here we show an example of one of the random replicas in Figure 9.

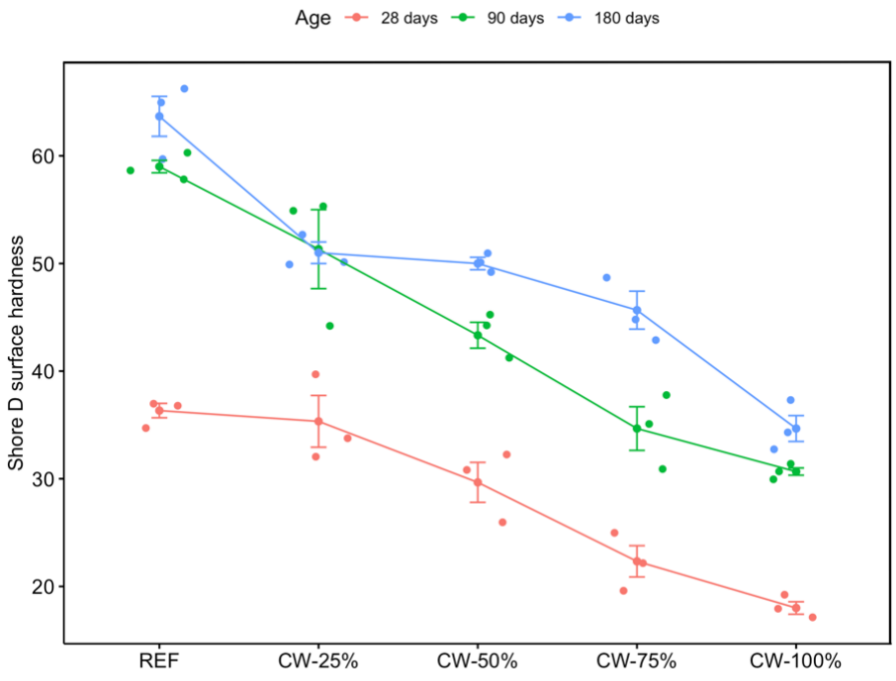

Figure 9. Random sample of shore D hardness values using only one measurement for each test tube. The dependence of the ANOVA model on dosage and age is significant ($p < 0.05$) across 100 random samples of the dataset.

3.2.3. Flexural and compressive strength Figures 10 and 11 show the flexural and compressive strength values obtained after the tests. For each test tube, measurements of flexural and were obtained. Three different tubes were formed for each age (three levels) and dosage (five levels) combination (3×5=15 possibilities), thus yielding 3×15 = 45 measurements overall. After carrying out flexural tests, specimens are broken into two pieces, yielding 6 independent samples for compressive strength. Out of those 6 new test tubes, we used 4 for compressive strength tests and the two remaining were used for other tests. This generates 3 x 5 x 4 = 60 values of compressive strength overall. For the mechanical characterization tests (Figure 10), the regulations do not establish a minimum reference value. As with surface hardness, flexural strength values increased as the days of sample processing increased, up to 129% in the reference test tubes and up to 85%-71%-83%-35%, respectively, in the mixtures with residues (CW-25% CW-50% CW-75% CW-100%), at 180 days. Comparing

the samples with the same manufacturing age, it may be observed that, at 28 days, the composites had lower average flexural strength values of 30%-37%-55%-63% with respect to the mean value of the flexural strength of the reference sample (1.2626 N/mm^2). At 90 days, these values imply a reduction of 45%-64%-75%-78%, respectively, out of the average reference value (2.7220 N/mm^2); and at 180 days, of 44%-53%-64%-78%, with average flexural strength values of 1.622 N/mm^2 (CW.25%), 1.358 N/mm^2 (CW-50%), 1.032 N/mm^2 (CW-75%), 0.637 N/mm^2 (CW-100%) with respect to the reference (2.2910 N/mm^2).

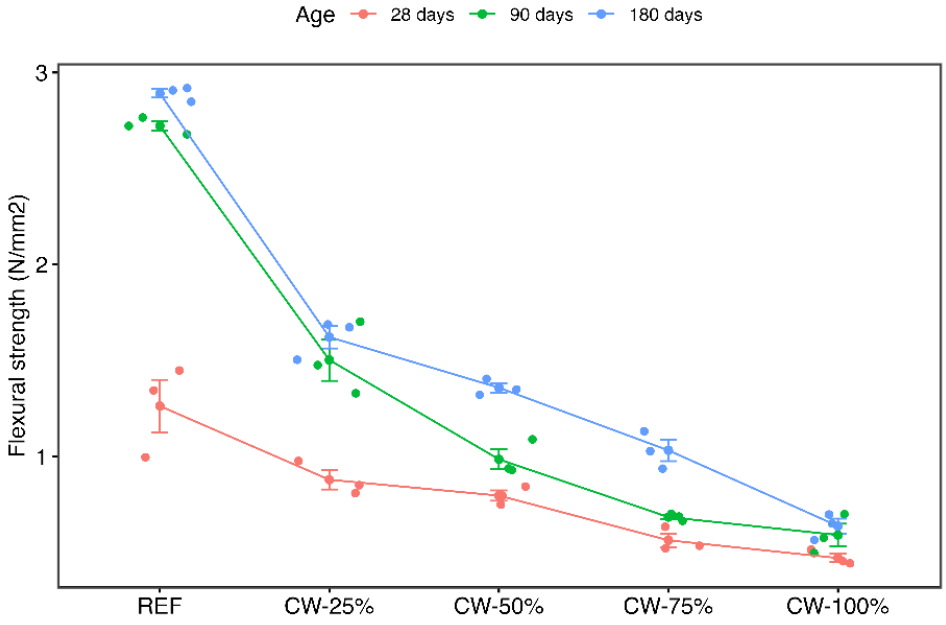

Figure 10. Flexural strength values of composites

The flexural strength was analyzed as a function of residue concentration and curing time using a two-way ANOVA with interaction. This model yielded significant p-values for both factors and for their interaction, indicating differences in flexural strength depending on residue concentration and curing time. The assumptions of homoscedasticity (Levene's test, p = 0.6576) and normality (Shapiro–Wilk test, p = 0.1736) were satisfied without data transformation. Consequently, it was not necessary to apply bootstrap-based two-way ANOVA variants, and the conclusions from the standard two-way ANOVA are reliable. These results support statistically significant differences in flexural strength across the different dosage levels and curing ages (see Figure 10).

Compressive strength (Figure 11) evolves in a manner similar to that of flexural strength, with the average values increasing as the days from their preparation increased, up to 287% in the reference specimens and up to 229%-245%-164%-106% respectively in the samples CW-25%, CW-50%, CW-75%, and CW-100%. However, on the contrary, they reduced their resistance as the polymer residue in the dosage increased. At 28 days, it is seen that the average compressive strength values decreased by 40%-48%-59%-70% as compared to the reference sample (1.7400 N/mm^2). At 90 days, this decrease was of 44%-66%-78%-82% with respect to the reference (5.3065 N/mm^2); and similarly, at 180 days, the reduction in the compressive strength of the reference sample was 49%-54%-72%-84% for the mixtures CW-25% CW-50% CW-75% CW-100%, with some average values of 3.411 N/mm^2 (CW.25%), 3.086 N/mm^2 (CW-50%), 1.909 N/mm^2 (CW-75%), 1.062 N/mm^2 (CW-100%) as compared to the reference (6.7400 N/mm^2).

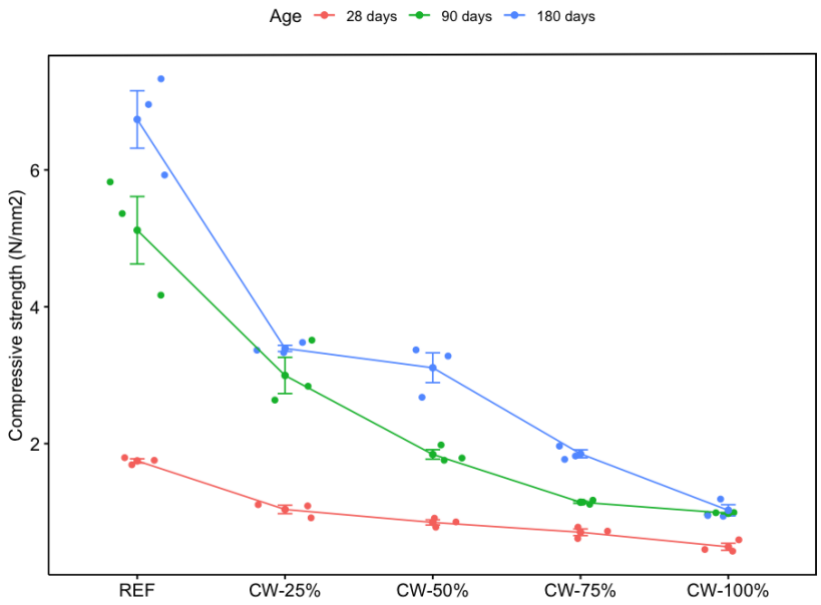

Figure 11. Compressive strength values of the composites

For compressive strength as a function of residue dosage, a standard two-way ANOVA was first applied. The normality assumption was not supported (Shapiro–Wilk test, $p = 1.901 \times 10^{-5}$), whereas homoscedasticity was not rejected (Levene's test, $p = 0.2096$). Since normality was violated, a two-way bootstrap ANOVA was used instead.

This bootstrap test indicated significant differences in compressive strength across dosage levels and for the interaction term ($p < 0.005$ for all three terms). As illustrated in Figure 11, the effect of dosage on compressive strength is decreasing. Thus, a significant effect of both age and dosage on compressive strength is obtained.

Although flexural and compressive strength decrease as the plastic aggregate content increases, mixtures with replacement levels of up to 75% still exhibit adequate mechanical performance for non-structural and/or lightweight applications (e.g., interior renders or non-load-bearing elements). This reflects a "good-enough" performance trade-off relevant to the circular-economy perspective, in which the mechanical capacity remains fit for purpose while circularity (higher recycled content and reduced use of natural sand) is substantially enhanced.

In light of the mechanical strength results, full (100%) replacement of natural sand is not recommended. The inclusion of such high substitution levels is intended to characterize the complete response of the material, rather than to propose these extreme mixtures as practical solutions. Mixtures with very high plastic contents are used to delineate the bounds of mechanical behaviour and to identify critical thresholds beyond which strength losses render the material unsuitable for most structural applications. These extreme formulations therefore act as boundary cases, enabling quantification of performance degradation and guiding the selection of more realistic replacement levels. Accordingly, mixtures exhibiting severe strength reductions (e.g., at or near 100% replacement) are reported to complete the analysis and enable comparison but are not put forward as viable options for practical implementation.

It is interesting to note that recent RILEM reviews show that lime-based binders harden through a coupled action of drying, carbonation, hydration of hydraulic phases and pozzolanic reactions, with their relative importance depending on whether the binder is air lime, natural hydraulic lime, or a lime–pozzolan / lime–cement blend (Alvarez et al., 2021). In air lime mortars, $Ca(OH)_2$ formed on slaking slowly carbonates as CO_2 diffuses inward in the presence of moisture, precipitating $CaCO_3$ in the pores; this diffusion-controlled carbonation, together with drying and pore refinement, governs stiffness and strength (Alvarez et al., 2021; Rodriguez-Navarro et al., 2023). Carbonation rate and microstructure depend strongly on relative humidity, CO_2 concentration, and lime fineness, and can be significantly accelerated by increased CO_2 or carbonation

promoters, which yield finer, denser $CaCO_3$ and higher early strength (Jia et al., 2024; Rodriguez-Navarro et al., 2023).

In natural hydraulic limes and lime–pozzolan systems, early setting is partly hydration-controlled (formation of C–S–H and related hydrates), but long-term strength still relies heavily on subsequent carbonation of portlandite and some hydrates, so hydration, pozzolanic reaction and carbonation proceed concurrently and competitively (Alvarez et al., 2021; Keppert et al., 2020). In contrast, Portland cement hardens primarily by hydration of alite and belite to form a space-filling C–S–H gel and portlandite, with minor AFt/AFm phases; mechanical behaviour is mainly controlled by the amount and connectivity of C–S–H (Zajac et al., 2022). Carbonation in cement is generally a later, durability-related process that decalcifies C–(A)–S–H and consumes portlandite, although under controlled curing it can also refine pores and add some strength through $CaCO_3$ precipitation (Siauciunas et al., 2025; Zajac et al., 2022).

3.2.4. Thermogravimetric analysis of the test tubes Hydraulic limes harden through two concurrent mechanisms that must be considered when interpreting thermogravimetric analysis (TGA) results (Garijo et al., 2020; Santos et al., 2018). First, carbonation of portlandite, $Ca(OH)_2$, with atmospheric CO_2 forms calcite, $CaCO_3$. Second, hydration of calcium silicates with water produces calcium silicate hydrates (CSH phase) and additional portlandite. During curing, a decrease in portlandite accompanied by an increase in calcite indicates progressive carbonation and improved mechanical properties.

In this work, portlandite and calcite contents were quantified by gravimetric thermal analysis (Grilo, Faria, et al., 2014; Vessalas et al., 2009), as has been shown in point 3.1.2 and Figure 4. Mass loss between 400–500 °C is attributed to the decomposition of $Ca(OH)_2$ to CaO and H_2O; using the 1:1 molar stoichiometry between $Ca(OH)_2$ and H_2O, the portlandite content was calculated. Similarly, mass loss between 500–800 °C corresponds to $CaCO_3$ decomposition to CaO and CO_2, allowing determination of calcite content based on the 1:1 molar ratio between $CaCO_3$ and CO_2.

Mechanical strength also develops through hydration of calcium silicates (e.g., larnite), as confirmed by XRD, forming CSH and portlandite. CSH may additionally form via pozzolanic reactions between portlandite and silica- or amorphous alumina-rich materials (e.g., sand aggregates and alumina-bearing lime compounds). An increase in CSH is generally correlated with improved mechanical properties. In this context, $Ca(OH)_2$ decreases with carbonation and pozzolanic CSH formation (Pacheco-Torgal et al., 2012; Vessalas et al., 2009), but increases when CSH forms by direct hydration of calcium silicates.

The CSH content was estimated by TGA from the mass loss between 100–400 °C, associated with dehydration/decomposition of CSH (superimposed on evaporation of residual free water near 100 °C) (Ferrández, Yedra, Atanes-Sánchez, et al., 2022; Ramachandran et al., 2002; Santos et al., 2018). Because CSH has variable stoichiometry, its absolute mass fraction cannot be computed, so a greater mass loss in this range was taken to indicate a higher CSH content.

Overall, three distinct mass-loss steps were evaluated in all samples (including CW-100% at 28 and 180 days) (Figure 12): (a) 100–400 °C for CSH decomposition, showing several overlapping events with DTG maxima around 140, 250, and 350 °C; (b) 400–500 °C for portlandite decomposition, with a DTG maximum near 425 °C, used to calculate $Ca(OH)_2$ and to track its consumption or formation depending on the dominant reaction; and (c) 500–800 °C for calcite decomposition, where higher calcite contents indicate higher carbonation and thus better mechanical performance. In this last range, two DTG humps at ~680 and ~720 °C were distinguished, attributed respectively to calcite formed by carbonation of portlandite and to calcite originally present in the raw lime. These three mass losses were quantified both in absolute (mg) and relative (%) terms for all mixtures and curing ages and used to derive the values reported in Tables 4–6.

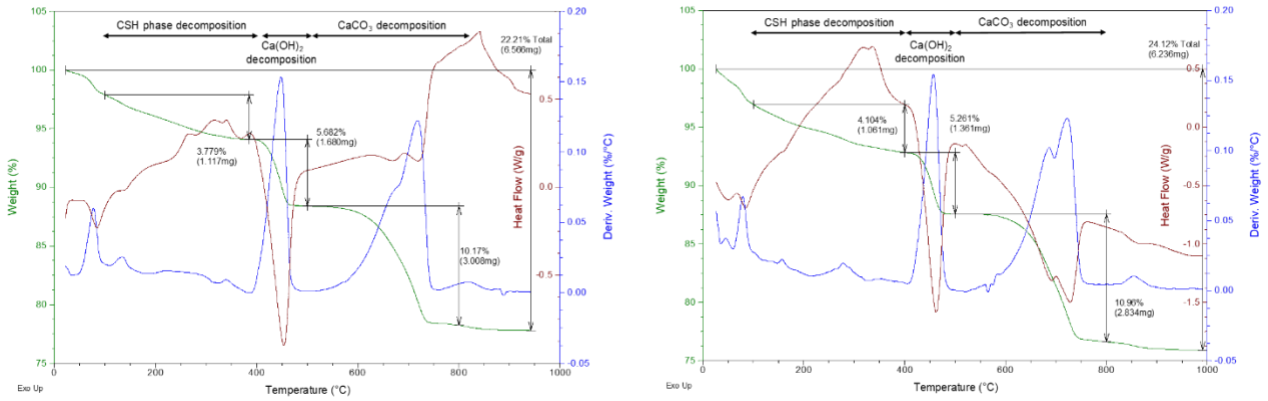

Figure 12. Thermogravimetric analysis of the sample CW-100% at 28 days (left) and 180 days (right).

Tables 4-5-6 are based on the thermal analyses of the test tube samples. Table 4 shows the mass losses associated with the thermal decomposition of CSH phase, since, as mentioned above, the variable stoichiometry of these hydrated compounds does not permit quantification of this phase. Tables 5 and 6 respectively show the mass of portlandite and calcite present in the samples, calculated as mentioned previously.

Table 4. Mass loss of the samples in the range 100-400ºC, corresponding to the thermal decomposition of CSH phase.

Age (days)	REF	CW-25%	CW-50%	CW-75%	CW-100%
28	2.948	2.915	2.818	3.178	3.780
90	3.722	3.346	3.612	4.593	5.424
180	3.436	3.600	3.681	3.729	4.104

Table 5. Percentage of portlandite $Ca(OH)_2$ in the samples calculated from the mass loss in the temperature range 400-500º C.

Age (days)	REF	CW-25%	CW-50%	CW-75%	CW-100%
28	16.57	14.65	16.11	18.89	23.64
90	16.69	14.74	17.10	20.82	22.27
180	14.07	15.27	18.26	20.15	21.89

Table 6. Percentage of calcite $CaCO_3$ in the samples calculated from the mass loss in the temperature range 500-800º C.

Age (days)	REF	CW-25%	CW-50%	CW-75%	CW-100%
28	8.23	16.08	17.23	20.73	23.30
90	14.34	14.08	15.60	18.66	22.68
180	10.94	16.59	16.27	18.69	25.10

As revealed in Table 4, over the 28–90-day period and using the criterion that higher mass loss by CSH dehydration indicates higher CSH content, all mixtures showed an increase in CSH phase, most markedly in REF, CW-75, and CW-100%, and more moderately in the 25% and 50% plastic waste mixes. Between 90 and 180 days, CSH content remained approximately constant in REF and in the 25% and 50% plastic waste samples but decreased sharply in the 75% and 100% plastic waste samples. Overall, from 28 to 180 days, CSH content increased in all mixes by 16.6%, 23.5%, 30.6%, 17.3%, and 8.6% for REF, CW-25%, CW-50%, CW-75%, and CW-100%, respectively. Since CSH may form both by hydration of calcium silicates and by pozzolanic consumption of portlandite, this age-related increase is consistent with the concurrent improvement in mechanical properties.

Lanas et al. (Lanas et al., 2004) reported a first hardening phase up to 28 days, governed by hydration and CSH formation, followed by a second phase up to ~182 days with only slight strength gain. In contrast, the present results show higher CSH contents at 90 and 180 days than at 28 days for all mixes, indicating that hydration-driven hardening persists beyond 28 days.

Portlandite shows, in Table 5, no consistent trend with age. From 28 to 180 days, its content decreases by 15.1% in REF and 7.4% in CW-100%, but increases by 4.2%, 13.3%, and 6.7% in CW-25%, CW-50%, and CW-75%, respectively. This is attributed to competing reactions: portlandite consumption by carbonation and pozzolanic CSH formation, and portlandite generation by calcium silicate hydration.

Calcite evolution is likewise complex (Table 6). In REF, calcite formed by portlandite carbonation increases by 32.9% from 28 to 180 days, indicating significant carbonation within this interval, earlier than suggested by Lanas (Lanas et al., 2004). Calcite also increases in CW-25% and CW-100% (by 3.2% and 7.7%) but decreases in CW-50% and CW-75% (by 5.6% and 9.8%). Nevertheless, at any given age, calcite content is higher in plastic-containing mixes than in REF, without corresponding strength improvement.

At a fixed age, increasing plastic content leads to higher CSH, calcite, and portlandite contents in the inorganic fraction. Since TGA is performed only on the sieved inorganic matrix, this suggests that both air-hardening (calcite formation) and hydraulic hardening (CSH formation) are enhanced in mixes with more plastic, likely due to increased pore volume (facilitating CO_2 ingress) and the hydrophobic character of plastic (favouring hydraulic reactions). However, despite the higher CSH and calcite contents, mechanical performance decreases with increasing plastic content. This discrepancy is explained by the fact that plastic particles are excluded from the thermal analysis but remain in the composite, where their low stiffness, poor adhesion to the matrix and the higher porosity they induce (voids and microcracks) weaken the overall structure. Previous studies similarly report that plastic waste addition increases porosity and reduces strength because of the low density and poor bonding of plastic inclusions, as also evidenced by SEM observations (Section 3.2.6) (Merlo et al., 2021; Soares et al., 2022).

It is important to clarify that (the TGA and XRD were obtained solely on the inorganic fraction of the material, after the plastic phase was removed, and the statement "reactions are favored in samples rich in plastic" should be interpreted exclusively in terms of the reactive matrix. This observation does not imply, in any case, an increase in the overall content of hydration products per unit volume of the compound, since the incorporation of plastic reduces (dilutes) the proportion of potentially reactive inorganic phase.

Overall, the CH/calcite data reflect that hydration and carbonation reactions remain highly active within the inorganic fraction of the lime matrix. However, the incorporation of plastic significantly alters the pore architecture and the quality of the paste-plastic and paste-aggregate interfaces. Consequently, hydration and carbonation processes can continue to progress in the inorganic phase, while the overall mechanical strength of the compound is primarily controlled by dilution effects of the reactive phase and by microstructural degradation phenomena (weakened transition zones and potential microcracks). This combination of mechanisms provides a coherent explanation for the apparent decoupling observed between the evolution of the chemical reactions (CH consumption and calcite formation) and the development of strength in plastic-modified mortars.

3.2.5. X-ray diffraction of the test tubes Figure 13 shows the X-ray diffractogram of the samples that incorporate 50% plastic residue at 28, 90, and 180 days.

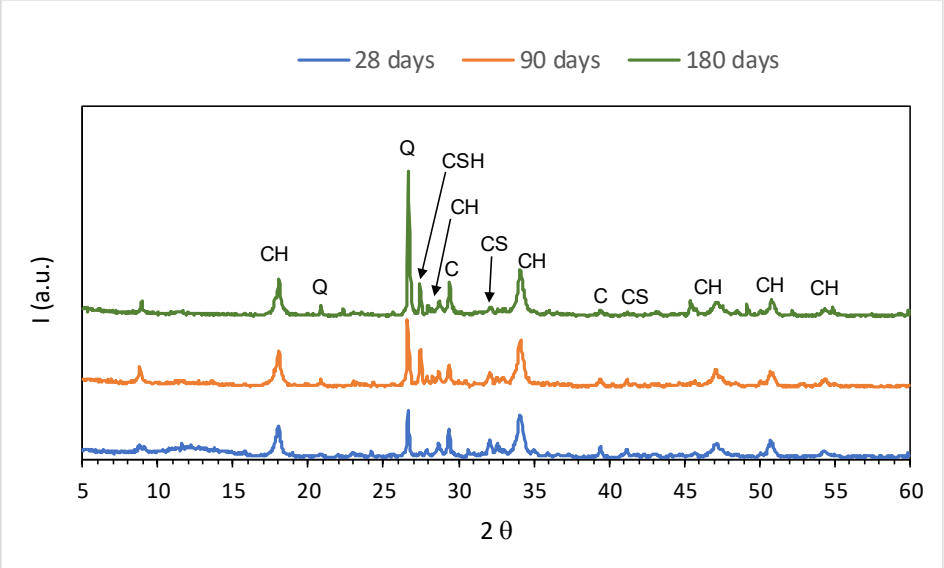

Figure 13. X-ray diffractogram of the sample CW-50% at 28 days, 90 days, and 180 days (CH: portlandite. C: calcium carbonate. CS: calcium silicate. Q: quartz. CSH: calcium silicate hydrate)

The portlandite, calcite, and quartz phases are identified, and the diffraction peaks corresponding to CSH phase appear at approximate values of 2θ of 26-27° and 27-28°, according to the results of the gravimetric thermal analysis. The calcium silicate peaks practically disappear at 180 days, which is consistent with their hydration, giving rise to CSH phase. On the other hand, the hydrated calcium silicate diffraction peaks, CSH phase, are more intense as the sample age increases.

3.2.6. Microscopy In Figure 14, different images obtained using the SEM technique at the reference age of 28 days are shown in a representative manner and to provide a better understanding of the microstructural behavior of the prepared mortars.

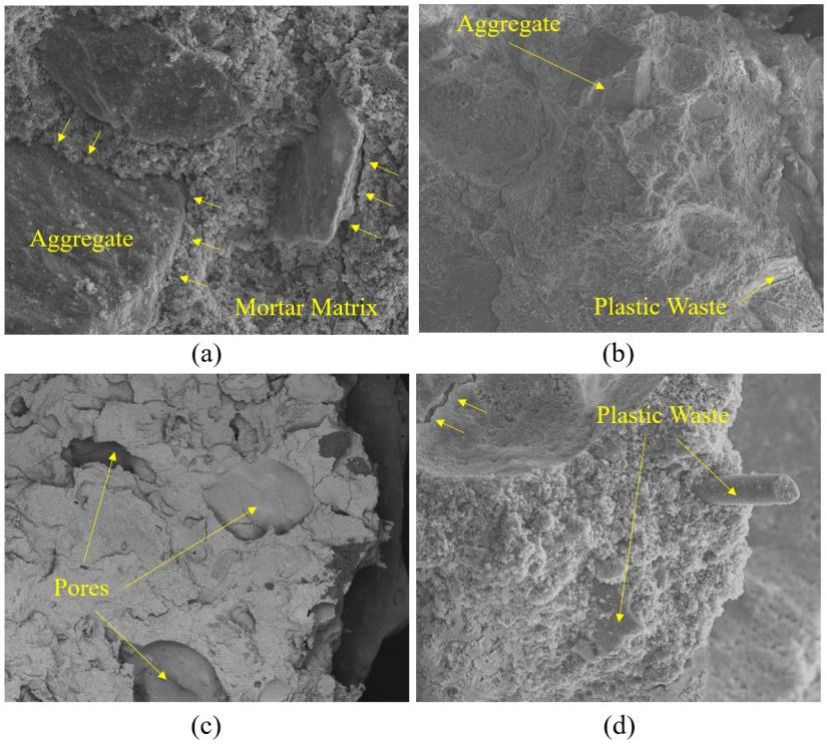

Figure 14. SEM analysis. (a) REF (500x zoom); (b) CW-50% (100x zoom); (c) CW-100% (20x zoom), and (d) CW-100% (500x zoom).

First, Figure 14(a) reveals good local adhesion between the natural aggregate and the matrix for the reference sample at 28 days. $CaCO_3$ crystals are seen to form at the aggregate-matrix interface, helping to prevent the sand from coming loose after failure in the flexural test. Figure 14(b) for the CW-50% sample shows how both types of aggregate, natural and electrical cable, and waste are perfectly adhered to the lime matrix and distributed over the observed surface. Figures 14(c) and 14(d) correspond to the sample prepared with 100% replacement of the natural aggregate with crushed plastic waste. In the first of these, greater porosity is observed in the mortar matrix. In addition, a more fragile matrix having multiple cracks distributed along its surface can be seen. Finally, Figure 14(d) shows in detail the good local adhesion between the plastic waste from the electrical cable and the prepared mortar matrix.

Although no chemical plasticizers were added, the progressive increase in plastic waste aggregate content modified the fresh-state rheology of the mortar. Due to its lower density and distinct surface texture compared with natural sand, the plastic phase altered aggregate packing and reduced internal friction within the granular skeleton. This change in particle arrangement made it possible to achieve the target workability with a lower water-to-binder ratio. However, the associated reduction in mixing water led to a higher volume fraction of capillary pores after setting and hardening, yielding a more open, less compact microstructure and a less efficient utilization of the available water for hydration reactions. These combined effects contributed to the observed loss of mechanical strength.

3.3. Circular economy perspective

These results should be interpreted within the broader trade-off inherent in circular building materials: increasing the plastic waste content improves the circularity of the system. In the lime-based composites studied that incorporate plastic waste, increasing the plastic content improves the circularity of the material and reduces density, but beyond an optimal replacement level, it leads to a marked reduction in compressive and flexural strength, as observed in other studies for cementitious composites and plastic waste (Álvarez et al., 2024; Messahel et al., 2023; Sabbrojjaman et al., 2024).

In line with recent approaches that use integrated indicators of circularity and performance (e.g. the Material Circularity Index and durability-specific indices) to capture such trade-offs (Masood Gholami & Hajikarimi, 2025; Mehmood et al., 2025; Montag & Pettau, 2023; Sanchez Moreno & Charter, 2025), the present work delineates “design windows” in which a modest loss of strength is considered acceptable in view of the gains in material circularity and environmental-impact reduction (Kılıç et al., 2024; Mehmood et al., 2025; Sun et al., 2025).

The proposed materials would be ideal for non-structural circular economy applications, such as prefabricated panels and restoration mortars. Other research also supports the suitability of these materials for the aforementioned applications, or even for insulating blocks (Acevedo-Sánchez et al., 2023; Ferrández, Yedra, Morón, et al., 2022). Furthermore, the incorporation of mineral wool in future research would improve flexural strength and durability against freeze-thaw cycles and salt crystallization, key properties for plastering and restoration mortars (Ferrández, Yedra, Morón, et al., 2022; Piña Ramírez et al., 2021). What is clear is that these compounds allow the valorization of plastic waste, the reduction of the use of virgin aggregates and binders and the decrease of the carbon footprint, in full harmony with the principles of the circular economy by transforming waste streams into high-value products for interior partitions, lightweight enclosures and rehabilitation mortars (Acevedo-Sánchez et al., 2023; Ferrández, Yedra, Morón, et al., 2022; Kountouris et al., 2025; Messahel et al., 2023).

At a system level, these findings suggest that substituting natural sand with cable-derived plastic aggregates in non-structural mortars could partly decouple construction material supply chains from primary sand extraction, alleviating local pressure on fluvial and coastal ecosystems. However, the practical contribution to sand demand reduction will ultimately depend on the availability and logistical integration of this specific waste stream, as well as on market uptake within existing standards and procurement practices. In addition, potential regulatory constraints on recycled content, quality assurance requirements and competing recycling routes for cable plastics may limit large-scale deployment, indicating that such mortars should be viewed as one complementary pathway within broader circular strategies for mineral resource management.

4. Conclusions

The incorporation of polymer waste as a sand substitute in lime mortars contributes to circular economy strategies by diverting plastics from landfill or incineration and reducing the extraction of natural aggregates. The use of polymer waste in lime mortars instead of sand improves the material's lightness, having a lower density and greater pore volume. However, other properties, such as flexural and compressive strength, are reduced. These results on the decrease in flexural and tensile strength with increasing proportion of plastic waste in the formulation are statistically significant. As for the influence of age on mechanical properties, in the studied range of 28, 90, and 180 days, flexural and compressive strength increased with age, in a statistically significant manner, although there was a lower level of significance as compared to the influence of composition.

The improvement in mechanical properties with age correlates well with the increase in the amount of CSH phase present in the calcareous mass of the samples as the curing time increases. This has been demonstrated by examining the chemical composition of the material through thermogravimetric analysis. No clear trend with age was found in the calcite content, which, together with CSH phase, is responsible for the mechanical strength of the samples. This may be because portlandite participates as a reagent in the pozzolanic reaction, which competes with the carbonation reaction of portlandite to form calcite. In fact, no clear evolution with age was revealed in the portlandite content. On the one hand, this appears to be due to its consumption as a reagent in these two reactions. And simultaneously, it was due to the formation of portlandite as a product in the hydration reaction of calcium silicates to form CSH phase.

On the other hand, thermogravimetric analysis revealed that, for samples of the same age, the percentage of CSH phase and calcite, the two compounds responsible for mechanical resistance, increases in the calcareous mass as the proportion of plastic waste in the sample increases. Considering that the thermogravimetric analysis was performed on the limestone mass, excluding plastic waste, it is evident that the presence of these wastes favors the aerial carbonation reactions to produce calcite and the hydraulic reactions of CSH phase formation. These favorable results may be attributed to the more porous structure resulting from the presence of plastic aggregates in the case of the carbonation reaction, and to their hydrophobicity in the case of CSH phase formation, in which H_2O participates. This calcareous mass with a higher proportion of CSH phase and calcite in the compounds having a higher content of plastic waste may provide improved mechanical properties to these compounds. However, this is not found to be the case, since, as discussed previously, it did not actually result in better mechanical properties. From a microstructural perspective, thermogravimetric analysis showed that, for mortars of the same age, higher contents of plastic waste increase the proportion of C–S–H phase and calcite in the calcareous matrix, indicating that these residues promote both hydraulic and carbonation reactions. This behavior suggests an enhanced capacity for CO_2 uptake and long-term mineral stabilization of carbon within the matrix, consistent with the role of lime-based binders as carbonating materials. Such behavior is advantageous in a circular economy context, where materials are expected not only to reuse waste but also to mitigate greenhouse gas emissions over their service life.

These seemingly contradictory results may be explained by the greater porosity, as well as the rounded geometry and/or short length of the polymer aggregates, which may weaken the composite structure. Thus, the greater pore volume and the poor interpenetration between the polymer aggregates and the calcareous mass cause the sample’s mechanical properties to decrease with the proportion of incorporated plastic waste. The coexistence of a strengthened calcareous matrix (higher C–S–H and calcite contents) with an overall loss of mechanical performance is attributed to the increased porosity and to the unfavorable geometry and limited interlocking of the rounded, short polymer particles. This points to the need for a design-oriented valorization of plastic waste—e.g., using waste-derived polymer fibers or tailored particle geometries—to reconcile resource efficiency, CO_2 reactivity, and mechanical performance. Consequently, lime mortars with polymer waste emerge as promising, circular-economy-compatible solutions for non-structural or lightweight applications, while future optimization of waste morphology and interfacial engineering could expand their structural and durability potential.

This leaves room for the possibility of studying other types of plastic wastes having distinct geometries, such as polymeric fibers from waste. These offer better cohesion to the whole by improving the interpenetration of the fiber with the calcareous mass. Therefore, they do not decrease or even increase the mechanical properties, while providing lightness and easy CO_2 access for the carbonation reaction.

In circular economy terms, these findings demonstrate that the proposed mortars can contribute to closing material loops in construction by diverting mixed plastic waste from landfill and reincorporating it as a secondary raw material. By partially replacing natural sand with bulk plastic waste at technically acceptable levels, the mixtures reduce dependence on virgin aggregates and help to alleviate pressure on primary sand extraction. Overall, this work positions mixed-plastic–lime mortars as a material-level enabler within broader circular economy transition strategies in the construction sector, providing evidence on feasible substitution ranges and performance trade-offs that can inform future system-level and policy interventions.

5. Implications

This work contributes to minimizing the environmental impact thanks to the reduction in the use of sand and water (raw materials) on the one hand, and, to the incorporation of polymer waste as a secondary raw material. The latter prevents its incineration and potential environmental contamination. As future lines of work, we propose studying the durability of these mortars and analyzing the effect on the physical and mechanical properties of freeze-thaw cycles or salt crystallization, among others. This would allow us to analyze their application possibilities in distinct geographical regions and explore their potential for the design of precast elements, which may be accompanied by an economic and life-cycle study.

6. Limitations

This study presents several limitations that affect the generalization of its findings. Only one hydraulic lime, a single aggregate gradation, and one family of polymeric residues with mainly rounded, short geometries were used, so the results cannot be directly extended to other binders, aggregate distributions, or plastic types. In addition, the plastic waste employed may contain different proportions of individual polymers and additives compared with other waste streams, which could influence its physical, chemical, and interfacial behavior in the composite. Therefore, the outcomes reported here should be interpreted as representative of the specific waste used, rather than universally applicable to all mixed plastic waste.

Curing and testing were restricted to 28, 90, and 180 days under controlled laboratory conditions, without assessing longer-term behavior or in-service environmental exposure. Thermogravimetric analysis was performed solely on the inorganic fraction after plastic removal, meaning the quantified CSH, portlandite, and calcite contents describe the calcareous matrix but not interfacial phenomena at the polymer–lime boundary. Mechanical characterization was limited to flexural and compressive strengths under monotonic loading, excluding fracture behavior, water transport, and durability under aggressive agents. Finally, only bulk polymer waste was evaluated as a sand replacement, and potentially beneficial alternatives such as surface-treated plastics or waste-derived polymer fibers with different geometries and enhanced interlocking were not investigated.

From a circular economy perspective, it is also important to acknowledge that this study does not include a life-cycle or techno-economic assessment of the proposed mixtures and therefore does not quantify environmental or economic circularity benefits in a systemic way. The analysis is instead confined to demonstrating material-level feasibility and potential for increased circularity in cementitious mortars, rather than optimising or fully validating circular economy performance across the value chain. These broader system-level assessments are beyond the scope of the present work and are envisaged for a subsequent phase of research.

7. Direction for Future Studies

In parallel, optimized mix designs and compatible additives should be explored to reinforce the interfacial transition zone without hindering carbonation, for example through partial sand replacement, polymer latexes, or fine mineral additions that refine pore structure and supply reactive silica or alumina. Advanced microstructural characterization (e.g. SEM, X-ray CT, MIP) is recommended to quantitatively relate porosity, ITZ quality and phase assemblage to mechanical behaviour over time.

Additionally, curing regimes and long-term performance deserve deeper investigation. Extended curing periods beyond 180 days, alternative curing environments (such as accelerated CO_2 curing or variable humidity/temperature), and realistic exposure conditions are needed to clarify the evolution of CSH, carbonates and portlandite and their impact on strength, durability and functional properties in non-structural and insulating mortars.

The development of prediction and optimization tools, such as response surface methodology and machine learning-based models, could support the identification of optimal combinations of polymer content, geometry, and curing conditions that balance lightness, porosity, carbonation efficiency, and mechanical performance for specific applications. Likewise, the study of surface treatments and coupling strategies (e.g., plasma/UV activation or PP fiber corona, or resin/silane-based coatings on plastic aggregates) would be a promising avenue for increasing surface energy and improving adhesion, and thus the flexural and compressive strength properties, of the proposed composites.

Finally, a life-cycle cost (LCC) analysis would make it possible to assess whether the costs of polymer surface treatments or CO_2 curing are offset by savings in raw materials, maintenance, and end-of-life management. In this way, the proposed prediction and optimization tools (RSM, ML) could be extended to couple mechanical responses with environmental and economic indicators, enabling the identification of trade-off solutions between lightness, strength, carbonation efficiency, and overall carbon footprint/life-cycle cost.

Acknowledgments This work has been supported by the Madrid Government (Comunidad de Madrid-Spain) under the Multiannual Agreement 2023-2026 with Universidad Politécnica de Madrid in the Line A, Emerging PhD researchers. The research is part of the Waste2BuildIns project («Waste processing to develop new environmentally sustainable construction products with improved mechanical and thermal properties») funded under this call.

Author Contributions Conceptualization, A.V. and D.F.; methodology, A.V, D.F., and E.A.; software, JA.C.; validation, A.V., D.F., E.A., and JA.C.; formal analysis, A.V., D.F., E.A., and JA.C.; investigation, A.V., D.F., E.A., and JA.C.; resources, A.V., D.F., and E.A.; data curation, A.V., and D.F.; writing—original draft preparation, A.V., D.F., E.A., and JA.C.; writing—review and editing, A.V., D.F., E.A., and JA.C.; visualization, A.V., D.F., E.A., and JA.C.; supervision, A.V.; project administration, A.V., and D.F.; funding acquisition, A.V., D.F., and E.A. All authors have read and agreed to the published version of the manuscript.

Data Availability The data on which this article is based is supported in https://github.com/jcapitan-upm/polymeric_waste, a national government page.

Declarations

Competing Interests The authors declare no competing interests.

References

Aattache, A. (2022). Properties and durability of partially replaced cement-based composite mortars co-using powders of a nanosilica superplasticiser and finely ground plastic waste. *Journal of Building Engineering*, *51*(March), 1–23. https://doi.org/10.1016/j.jobe.2022.104257

Abadian, M., & Russell, J. D. (2024). Exploring Backcasting as a Tool to Co-create a Vision for a Circular Economy: A Case Study of the Polyurethane Foam Industry. *Journal of Circular Economy*, *2*(2). https://doi.org/10.55845/UZXQ5070

Acevedo-Sánchez, C. D., Villaquirán-Caicedo, M. A., & Marmolejo-Rebellón, L. F. (2023). Recycling of eps foam and demolition wastes in the preparation of ecofriendly render mortars with thermal-acoustic insulation properties. *Materiales de Construcción*, *73*(351), e317. https://doi.org/10.3989/mc.2023.342422

Aciu, C., Ilutiu-Varvara, D. A., Manea, D. L., Orban, Y. A., & Babota, F. (2018). Recycling of plastic waste materials in the composition of ecological mortars. *Procedia Manufacturing*, *22*, 274–279. https://doi.org/10.1016/j.promfg.2018.03.042

AENOR. (2007). *UNE-EN 1015-2 Métodos de ensayo de los morteros para albañilería. Parte 2: Toma de muestra total de morteros y preparación de los morteros para ensayo* (p. 10). AENOR Asociación Española de Normalización y Certificación.

AENOR. (2016). *UNE-EN 459-1 Cales para la construcción. Parte 1: Definiciones, especificaciones y criterios de conformidad* (p. 50). AENOR Asociación Española de Normalización y Certificación.

Ahmed, N. (2023). Utilizing plastic waste in the building and construction industry : A pathway towards the circular economy. *Construction and Building Materials*, *383*(April), 131311. https://doi.org/10.1016/j.conbuildmat.2023.131311

Aldaou, L., Issaadi, N., Leklou, N., & Amiri, O. (2025). Thermal properties of recycled plastics waste/hemp shive composites. *Journal of Building Engineering*, *108*, 112885. https://doi.org/10.1016/j.jobe.2025.112885

Al-Noaimat, Y. A., Sambucci, M., Chougan, M., El-Seidy, E., Biblioteca, I., Valente, M., Tirillò, J., Al-Kheetan, M. J., Ghaffar, S. H., & Ghaffar. (2025). Sustainable repurposing of polyvinyl chloride waste as aggregates in limestone-calcined clay cement. *Journal of Cleaner Production*, *491*, 144862. https://doi.org/10.1016/j.jclepro.2025.144862

Alvarez, J. I., Veiga, R., Martinez-Ramirez, S., Secco, M., Faria, P., Maravelaki, P. N., Ramesh, M., Papayianni, I., & Va´lek, J. (2021). RILEM TC 277-LHS report: a review on the mechanisms of setting and hardening of lime-based binding systems. *Materials and Structures*, *54*(63). https://doi.org/10.1617/s11527-021-01648-3(0123456789().,-volV)(01234567

Álvarez, M., Ferrández, D., Zaragoza-Benzal, A., & Colorado-Pastor, B. (2024). Initiative to Increase the Circularity of HDPE Waste in the Construction Industry: A Physico-Mechanical Characterization of New Sustainable Gypsum Products. *Applied Sciences*, *14*(2), 478. https://doi.org/10.3390/app14020478

Amenta, M., Karatasios, I., Maravelaki-Kalaitzaki, P., & Kilikoglou, V. (2017). The role of aggregate characteristics on the performance optimization of high hydraulicity restoration mortars. *Construction and Building Materials*, *153*, 527–534. https://doi.org/10.1016/j.conbuildmat.2017.07.134

Apostolopoulou, M., Bakolas, A., & Kotsainas, M. (2021). Mechanical and physical performance of natural hydraulic lime mortars. *Construction and Building Materials*, *290*, 123272. https://doi.org/10.1016/j.conbuildmat.2021.123272

Athira, V. S., & Manohar, S. (2023). Carbonation of air lime mortars under natural and accelerated conditions – A systematic review. *Materials Today: Proceedings*, *xxxx*. https://doi.org/10.1016/j.matpr.2023.04.082

Piña Ramírez, C., del Río Merino, M., Vñas Arrebola, C., Vidales-Barriguete, A., & Aguilera Benito, P. (2021). Durability of cement mortars reinforced with insulation waste from the construction industry. *Journal of Building Engineering*, *40*, 102719. https://doi.org/10.1016/j.jobe.2021.102719

Chen, H., Qin, R., Lun, C., & Lau, D. (2023). Recycling thermoset plastic waste for manufacturing green cement mortar. *Cement and Concrete Composites*, *137*(October 2022), 104922. https://doi.org/10.1016/j.cemconcomp.2022.104922

Ferrández, D., Saiz, P., Zaragoza-Benzal, A., & Zúñiga-Vicente, J. A. (2023). Towards a more sustainable environmentally production system for the treatment of recycled aggregates in the construction industry: An experimental study. *Heliyon*, *9*(6). https://doi.org/10.1016/j.heliyon.2023.e16641

Ferrández, D., Yedra, E., Atanes-Sánchez, E., & Morón, C. (2022). Arduino based monitoring system for materials used in façade rehabilitation − Experimental study with lime mortars. *Case Studies in Construction Materials*, *16*. https://doi.org/10.1016/j.cscm.2022.e00985

Ferrández, D., Yedra, E., Morón, C., Zaragoza, A., & Kosior-Kazberuk, M. (2022). Circular Building Process: Reuse of Insulators from Construction and Demolition Waste to Produce Lime Mortars. *Buildings*, *12*(2), 220. https://doi.org/10.3390/buildings12020220

Ferrández, D., Zaragoza-Benzal, A., Carballosa, P., García Calvo, J. L., & Santos, P. (2025). Gypsum-Based Composites with Recycled PP/HDPE Pellets for Circular Material Development: A Comprehensive Characterisation. *Materials*, *18*(17), 4037. https://doi.org/10.3390/ma18174037

Fritz Benachio, G. L., Duarte Freitas, M. do C., & Tavare, S. F. (2020). Circular economy in the construction industry: A systematic literature review. *Journal of Cleaner Production*, *260*, 121046. https://doi.org/10.1016/j.jclepro.2020.121046

García-Gutiérrez, P., Martino Amadei, A., Klenert, D., Nessi, S., Tonini, D., Tosches, D., Ardente, F., & Saveyn, H. G. M. (2025). Environmental and economic assessment of plastic waste recycling and energy recovery pathways in the EU. *Resources, Conservation and Recycling*, *215*, 108099. https://doi.org/10.1016/j.resconrec.2024.108099

Garijo, L., Zhang, X., Ruiz, G., & Ortega, J. J. (2020). Age effect on the mechanical properties of natural hydraulic and aerial lime mortars. *Construction and Building Materials*, *236*. https://doi.org/10.1016/j.conbuildmat.2019.117573

Garijo, L., Zhang, X., Ruiz, G., Ortega, J. J., & Wu, Z. (2018). The effects of dosage and production process on the mechanical and physical properties of natural hydraulic lime mortars. *Construction and Building Materials*, *169*, 325–334. https://doi.org/10.1016/j.conbuildmat.2018.03.016

Geng, X., Song, N., Zhao, Y., & Zhou, T. (2022). Waste plastic resource recovery from landfilled refuse : A novel waterless cleaning method and its cost-benefit analysis. *Journal of Environmental Management*, *306*(January), 114462. https://doi.org/10.1016/j.jenvman.2022.114462

Ghaffar, S. H., Burman, M., & Braimah, N. (2020). Pathways to circular construction: An integrated management of construction and demolition waste for resource recovery. *Journal of Cleaner Production*, *244*, 118710. https://doi.org/10.1016/j.jclepro.2019.118710

Gil, L., Bernat-Masó, E., & Cañavate, F. J. (2016). Changes in properties of cement and lime mortars when incorporating fibers from end-of-life tires. *Fibers*, *4*(1), 1–13. https://doi.org/10.3390/fib4010007

Ginga, C. P., Ongpeng, J. M. C., & M. Daly, Ma. K. (2020). Circular Economy on Construction and Demolition Waste: A Literature Review on Material Recovery and Production. *Materials*, *13*(13), 2970. https://doi.org/10.3390/ma13132970

Grilo, J., Faria, P., Veiga, R., Santos Silva, A., Silva, V., & Velosa, A. (2014). New natural hydraulic lime mortars - Physical and microstructural properties in different curing conditions. *Construction and Building Materials*, *54*, 378–384. https://doi.org/10.1016/j.conbuildmat.2013.12.078

Grilo, J., Silva, A. S., Faria, P., Gameiro, A., Veiga, R., & Velosa, A. (2014). Mechanical and mineralogical properties of natural hydraulic lime-metakaolin mortars in different curing conditions. *Construction and Building Materials*, *51*, 287–294. https://doi.org/10.1016/j.conbuildmat.2013.10.045

Hamieh, N., Florence, C., & Amina, M. (2024). An innovative drying method for on-site and precast walls – Efficiency in accelerating the drying of reduced-scale earth-lime-hemp composites. *Construction and Building Materials*, *431*, 136587. https://doi.org/10.1016/j.conbuildmat.2024.136587

Herrero, S., Mayor, P., & Hernández-Olivares, F. (2013). Influence of proportion and particle size gradation or rubber from end-of-life tires on mechanical, thermal and acoustic properties of plaster-rubber mortars. *Materials & Design*, *47*, 633–642. https://doi.org/10.1016/j.matdes.2012.12.063

Iucolano, F., Liguori, B., Caputo, D., Colangelo, F., & Cioffi, R. (2013). Recycled plastic aggregate in mortars composition: Effect on physical and mechanical properties. *Materials & Design (1980-2015)*, *52*, 916–922. https://doi.org/10.1016/j.matdes.2013.06.025

Jerónimo, A., Soares, C., Aguiar, B., & Lima, N. (2020). Hydraulic lime mortars incorporating micro cork granules with antifungal properties. *Construction and Building Materials*, *255*. https://doi.org/10.1016/j.conbuildmat.2020.119368

Jia, M., Zhao, Y., Wu, X., & Ma, X. (2024). The effect of carbonation accelerator on enhancing the carbonation process and mechanical strength of air-hardening lime mortars. *Construction and Building Materials*, *425*, 136067. https://doi.org/10.1016/j.conbuildmat.2024.136067

Keppert, M., Scheinherrová, L. K. L., Doleželová, M., Brus, J., & Černý, R. (2020). Kinetics of pozzolanic reaction and carbonation in ceramic – lime system: Thermogravimetry and solid-state NMR spectroscopy study. *Journal of Building Engineering*, *32*, 101729. https://doi.org/10.1016/j.jobe.2020.101729

Kılıç, E., Fullana-i-Palmer, P., Fullana, M., Delgado-Aguilar, M., & Puig, R. (2024). Circularity of new composites from recycled high density polyethylene and leather waste for automotive bumpers. Testing performance and environmental impact. *Science of the Total Environment*, *919*, 170413. https://doi.org/10.1016/j.scitotenv.2024.170413

Kountouris, A., Efstathiou, K., Kostoglou, N., Manolakos, D., & Rebholz, C. (2025). A New Recycling Technology to Produce Premixed Thermal Insulating Mortars from Polyurethane Waste Foams. *Polymers*, *17*(176), 2233. https://doi.org/10.3390/polym17162233

Kulas, D. G., Zolghadr, A., Chaudhari, U. S., & Shonnard, D. R. (2023). *Economic and environmental analysis of plastics pyrolysis after secondary sortation of mixed plastic waste*. *384*(September 2022).

Lamba, P., Kaur, D. P., Raj, S., & Sorout, J. (2021). Recycling/reuse of plastic waste as construction material for sustainable development: a review. *Environmental Science and Pollution Research*, *29*, 86156–86179. https://doi.org/10.1007/s11356-021-16980-y

Lanas, J., Bernal, J. L. P., Bello, M. A., & Galindo, J. I. A. (2004). Mechanical properties of natural hydraulic lime-based mortars. *Cement and Concrete Research*, *34*(12), 2191–2201. https://doi.org/10.1016/j.cemconres.2004.02.005

Lazorenko, G., Kasprzhitskii, A., & Fini, E. H. (2022). Polyethylene terephthalate (PET) waste plastic as natural aggregate replacement in geopolymer mortar production. *Journal of Cleaner Production*, *375*(March), 134083. https://doi.org/10.1016/j.jclepro.2022.134083

López Ruiz, L. A., Roca Ramón, X., & Gassó Domingo, S. (2020). The circular economy in the construction and demolition waste sector – A review and an integrative model approach. *Journal of Cleaner Production*, *248*, 119238. https://doi.org/10.1016/j.jclepro.2019.119238

Loureiro, A. M. S., Paz, S. P. A., Veiga, M. do R., & Angélica, R. S. (2020). Assessment of compatibility between historic mortars and lime-METAKAOLIN restoration mortars made from amazon industrial waste. *Applied Clay Science*, *198*(February), 105843. https://doi.org/10.1016/j.clay.2020.105843

Malathy, R., Shanmugam, R., Dhamotharan, D., Kamaraj, D., Prabakaran, M., & Kim, J. (2023). Lime based concrete and mortar enhanced with pozzolanic materials – State of art. *Construction and Building Materials*, *390*, 131415. https://doi.org/10.1016/j.conbuildmat.2023.131415

Masood Gholami, A. K., & Hajikarimi, P. (2025). A multifaceted purpose-oriented approach to evaluate material circularity index for rejuvenated recycled asphalt mixtures. *Scientific Reports*, *15*, 12213. https://doi.org/10.1038/s41598-025-96749-2

Meddah, M. S., Al Owaisi, M., Abedi, M., & Hago, A. W. (2023). Mortar and concrete with lime-rich calcined clay pozzolana: A sustainable approach to enhancing performances and reducing carbon footprint. *Construction and Building Materials*, *393*(May), 132098. https://doi.org/10.1016/j.conbuildmat.2023.132098

Mehmood, M., Nie, W., Manan, A., Onyelowe, K. C., & Arunachalan, K. P. (2025). Life cycle assessment of eco-friendly high performance cementitious composites incorporating construction and industrial waste. *Scientific Reports*, *15*, 37113. https://doi.org/10.1038/s41598-025-21151-x

Meng, J., Zhou, Y., Li, D., & Jiang, X. (2023). Degradation of plastic wastes to commercial chemicals and monomers under visible light. *Science Bulletin*, *68*(14), 1522–1530. https://doi.org/10.1016/j.scib.2023.06.024

Merlo, A., Lavagna, L., Suarez-Riera, D., & Pavese, M. (2020). Mechanical properties of mortar containing waste plastic (PVC) as aggregate partial replacement. *Case Studies in Construction Materials*, *13*, e00467. https://doi.org/10.1016/j.cscm.2020.e00467

Merlo, A., Lavagna, L., Suarez-Riera, D., & Pavese, M. (2021). Recycling of WEEE Plastics Waste in Mortar: The Effects on Mechanical Properties. *Recycling*, *6*(4), 70. https://doi.org/10.3390/recycling6040070

Messahel, B., Onyenokporo, N., Takyie, E., Beizaee, A., & Oyinlola, M. (2023). Upcycling agricultural and plastic waste for sustainable construction: a review. *Environmental Technology Reviews*, *12*(1), 37–59. https://doi.org/10.1080/21622515.2023.2169642

Mohamad, S. A., Adel, A., Al-hamd, R. K. S., & Alzabeebee, S. (2024). *Materials Today : Proceedings The production of novel sustainable lightweight mortar from the electronic plastic waste*. *xxxx*.

Moletti, C., Aversa, P., Losini, A. E., Dotelli, G., Woloszyn, M., & Luprano, V. A. M. (2023). Hygrothermal behaviour of hemp-lime walls: the effect of binder carbonation over time. *Building and Environment*, *233*(September 2022), 110129. https://doi.org/10.1016/j.buildenv.2023.110129

Montag, L., & Pettau, T. (2023). Process Performance Measurement Framework For Circular Supply Chains: An Updated SCOR Perspective. *Journal of Circular Economy*, *1*(1). https://doi.org/10.55845/KAIZ3670

Mosquera, M. J., Silva, B., Prieto, B., & Ruiz-Herrera, E. (2006). Addition of cement to lime-based mortars: Effect on pore structure and vapor transport. *Cement and Concrete Research*, *36*(9), 1635–1642. https://doi.org/10.1016/j.cemconres.2004.10.041

Nassiri, O., Mahboub, I., Ibnoussina, M., Moukmir, O., Amrani, A. El, Mazirh, K., Ammari, A., & Cheickine, I. El. (2024). Physico-mechanical, structural, and mineralogical analysis of composite concrete incorporating hydraulic lime and pozzolan. *Construction and Building Materials*, *437*, 136804. https://doi.org/10.1016/j.conbuildmat.2024.136804

Norouzi, M., Chàfer, M., Cabeza, L. F., Jiménez, L., & Boer, D. (2021). Circular economy in the building and construction sector: A scientific evolution analysis. *Journal of Building Engineering*, *44*, 102704. https://doi.org/10.1016/j.jobe.2021.102704

Ogunmakinde, O. E. (2024). The Circular Economy in the Construction Industry: From Research to Practice. *Journal of Circular Economy*, *2*(3). https://doi.org/10.55845/DHNN3429

Pacheco-Torgal, F., Faria, J., & Jalali, S. (2012). Some considerations about the use of lime-cement mortars for building conservation purposes in Portugal: A reprehensible option or a lesser evil? *Construction and Building Materials*, *30*, 488–494. https://doi.org/10.1016/j.conbuildmat.2011.12.003

Purchase, C. K., Zulayq, D. M. Al, O'Brien, B. T., Kowalewski, M. J., Berenjian, A., Tarighaleslami, A. H., & Seifan, M. (2022). Circular Economy of Construction and Demolition Waste: A Literature Review on Lessons, Challenges, and Benefits. *Materials*, *15*(1), 76. https://doi.org/10.3390/ma15010076

Raeis Samiei, R., Daniotti, B., Pelosato, R., & Dotelli, G. (2015). Properties of cement-lime mortars vs. cement mortars containing recycled concrete aggregates. *Construction and Building Materials*, *84*, 84–94. https://doi.org/10.1016/j.conbuildmat.2015.03.042

Ramachandran, V. S., Paroli, R. M., Beaudoin, J. J., & Delgado, A. H. (2002). Formation and Hydration of Cement and Cement Compounds. *Handbook of Thermal Analysis of Construction Materials*, 71–142. https://doi.org/10.1016/b978-081551487-9.50005-0

Rani, S. D., Rahul, A. V., & Santhanam, M. (2021). A multi-analytical approach for pore structure assessment in historic lime mortars. *Construction and Building Materials*, *272*, 121905. https://doi.org/10.1016/j.conbuildmat.2020.121905

Rathore, R. S., Chouhan, H. S., & Prakash, D. (2021). Influence of plastic waste on the performance of mortar and concrete: A review. *Materials Today: Proceedings*, *47*, 4708–4711. https://doi.org/10.1016/j.matpr.2021.05.603

Resende, D. M., Mendes, V. F., Carvalho, V. R., Auiar Nogueira, M., Franco de Carvalho, J. M., & Fiorotti Peixoto, R. A. (2024). Coating mortars produced with recycled PET aggregates: A technical, environmental, and socioeconomic approach applied to Brazilian social housing. *Journal of Building Engineering*, *83*, 108426. https://doi.org/10.1016/j.jobe.2023.108426

Rodriguez-Navarro, C., Ilić, T., Ruiz-Agudo, E., & Elert, K. (2023). Carbonation mechanisms and kinetics of lime-based binders: An overview. *Cement and Concrete Research*, *173*, 107301. https://doi.org/10.1016/j.cemconres.2023.107301

Sabbrojjaman, M., Liu, Y., & Tafsirojjaman, T. (2024). A comparative review on the utilisation of recycled waste glass, ceramic and rubber as fine aggregate on high performance concrete: Mechanical and durability properties. *Developments in the Built Environment*, *17*, 100371. https://doi.org/10.1016/j.dibe.2024.100371

Safi, B., Saidi, M., Aboutaleb, D., & Maallem, M. (2013). The use of plastic waste as fine aggregate in the self-compacting mortars: Effect on physical and mechanical properties. *Construction and Building Materials*, *43*, 436–442. https://doi.org/10.1016/j.conbuildmat.2013.02.049

Sanchez Moreno, L., & Charter, M. (2025). Assessing Product Circularity in Practice: Insights from Industry. *Journal of Circular Economy*, *3*(3). https://doi.org/10.55845/TEFD6720

Santos, A. R., Veiga, M. do R., Santos Silva, A., de Brito, J., & Álvarez, J. I. (2018). Evolution of the microstructure of lime based mortars and influence on the mechanical behaviour: The role of the aggregates. *Construction and Building Materials*, *187*, 907–922. https://doi.org/10.1016/j.conbuildmat.2018.07.223

Siauciunas, R., Smigelskyte, A., & Aliukonyte, N. (2025). Factors Influencing the Carbonation Kinetics of Calcium Silicate-Based Binders—An Overview. *Sustainability*, *17*, 4191. https://doi.org/10.3390/su17094191

Soares, I., Nobre, F. X., Vasconcelos, R., & Ramírez, M. A. (2022). Study of Metakaolinite Geopolymeric Mortar with Plastic Waste Replacing the Sand: Effects on the Mechanical Properties, Microstructure, and Efflorescence. *Materials*, *15*(23), 8626. https://doi.org/10.3390/ma15238626

Stefanidou, M., Anastasiou, E., & Georgiadis Filikas, K. (2014). Recycled sand in lime-based mortars. *Waste Management*, *34*(12), 2595–2602. https://doi.org/10.1016/j.wasman.2014.09.005

Sun, F., Lu, C., Zhang, Z., Abdalla, J. A., Hawileh, R. A., & Zhang, X. (2025). High strength Engineered Cementitious Composites (ECC) with recycling waste glass powder: Mechanical properties and environmental benefits. *Case Studies in Construction Materials*, *22*, e04380. https://doi.org/10.1016/j.cscm.2025.e04380

Syed Nasir, A., & Qureshi, M. I. (2025). Effect of recycled plastic aggregates on mechanical and durability properties of concrete: A review. *Materials Chemistry and Physics: Sustainability and Energy*, *3*, 100016. https://doi.org/10.1016/j.macse.2025.100016

Tang, Z., Zhang, H., Pan, Y., Ke, L., Xiang, Z., & Lai, Z. (2023). Experimental study on mechanical properties of basalt Fiber-Clay lime mortar and application in brick masonry. *Construction and Building Materials*, *398*(July), 132479. https://doi.org/10.1016/j.conbuildmat.2023.132479

Tejaswini, M. S. S. R., Pathak, P., Ramkrishna, S., & Ganesh, P. S. (2022). Science of the Total Environment A comprehensive review on integrative approach for sustainable management of plastic waste and its associated externalities. *Science of the Total Environment*, *825*, 153973. https://doi.org/10.1016/j.scitotenv.2022.153973

UNE. (2018). *UNE-EN 196-1 Métodos de ensayo de cementos. Parte 1: Determinación de resistencias* (p. 40). Asociación española de normalización.

UNE. (2020). *UNE-EN 1015-11 Métodos de ensayo de los morteros para albañilería. Parte 11: Determinación de la resistencia a flexión y a compresión del mortero endurecido* (p. 20). UNE Normalización española.

UNE-EN 13279-2:2014. (2014). *Yesos de construcción y conglomerantes a base de yeso para la construcción. Parte 2: Métodos de ensayo*.

Vanderschelden, B., Bossche, R. Van den, Bossche, N. Van Den, Cnudde, V., & Kock, T. De. (2024). The impact of lime as a replacement of cement-based mortar, on the water absorption and rain penetration of masonry. *MATEC Web Conf*, *403*, 05012. https://doi.org/10.1051/matecconf/202440305012

Vessalas, K., Thomas, P. S., Ray, A. S., Guerbois, J., Joyce, P., & Haggman, J. (2009). *Vessalas2009*. *97*, 71–76.

Vidales Barriguete, A. (2019). *Caracterización fisicoquímica y aplicaciones de yeso con adición de residuo plástico de cables mediante criterios de economía circular* [Tesis Doctoral, Universidad Politécnica de Madrid (España)]. https://doi.org/10.20868/UPM.thesis.57437

Vidales Barriguete, A., del Río Merino, M., Atanes Sánchez, E., Piña Ramírez, C., & Viñas Arrebola, C. (2018). Analysis of the feasibility of the use of CDW as a low-environmental-impact aggregate in conglomerates. *Construction and Building Materials*, *178*, 83–91. https://doi.org/10.1016/j.conbuildmat.2018.05.011

Vidales-Barriguete, A., Atanes-Sánchez, E., del Río-Merino, M., & Piña-Ramírez, C. (2020). Analysis of the improved water-resistant properties of plaster compounds with the addition of plastic waste. *Construction and Building Materials*, *230*, 116956. https://doi.org/10.1016/j.conbuildmat.2019.116956

Wang, Z., Hostikka, S., & Wang, J. (2022). Case Studies in Thermal Engineering Pyrolysis behavior and kinetic analysis of waste polypropylene-based complex for cable filler. *Case Studies in Thermal Engineering*, *37*(June), 102261. https://doi.org/10.1016/j.csite.2022.102261

Xue, C., Thew, E., Sen, Z., Srinophakun, P., & Wei, C. (2023). Bioresource Technology Recent advances and challenges in sustainable management of plastic waste using biodegradation approach. *Bioresource Technology*, *374*(February), 128772. https://doi.org/10.1016/j.biortech.2023.128772

Zajac, M., Irbe, L., Bullerjahn, F., Hilbig, H., & Haha, M. Ben. (2022). Mechanisms of carbonation hydration hardening in Portland cements. *Cement and Concrete Research*, *152*, 106687. https://doi.org/10.1016/j.cemconres.2021.106687

Zaragoza-Benzal, A., Ferrández, D., Atanes-Sánchez, E., & Morón, C. (2023). New lightened plaster material with dissolved recycled expanded polystyrene and end-of-life tyres fibres for building prefabricated industry. *Case Studies in Construction Materials*, *18*(October 2022). https://doi.org/10.1016/j.cscm.2023.e02178

Zhu, J., Zhang, R., Zhang, Y., & He, F. (2019). The fractal characteristics of pore size distribution in cement-based materials and its effect on gas permeability. *Scientific Reports*, *9*, 17191. https://doi.org/10.1038/s41598-019-53828-5

Zulkernain, N. H., Gani, P., Chuan, N. C., & Uvarajan, T. (2021). Utilisation of plastic waste as aggregate in construction materials: A review. *Construction and Building Materials*, *296*, 123669. https://doi.org/10.1016/j.conbuildmat.2021.123669